Process Integration and Optimization for Sustainability
https://doi.org/10.1007/s41660-024-00395-6

ORIGINAL RESEARCH PAPER

Optimisation of Vacuum Distillation Units in Oil Refineries Using Surrogate Models

Shi Xie H'ng[1] · Lik Yin Ng[2] · Denny K. S. Ng[2,3] · Viknesh Andiappan[4]

Received: 26 February 2023 / Revised: 24 November 2023 / Accepted: 10 January 2024

Abstract
To ensure the optimum performance of downstream processes in a petrochemical refinery, the operation of a vacuum distillation unit (VDU) is critical. It needs to satisfy the yield and quality requirements of the downstream process. Otherwise, it will result in a loss of profitability in the refinery. Hence, it is important to optimise the operation of the VDU to ensure optimum performance. Traditionally, VDU is operated within the design envelope, and its operation condition is fine-tuned based on the operator's experience. However, such action does not guarantee the optimum performance of the entire refinery as it only considers the operation of VDU without understanding the effects towards downstream processes. Therefore, this work presents a framework to optimise VDU operations with consideration of the downstream processes. The framework consists of process simulation, surrogate modelling, and multi-objective optimisation. The developed framework aims to determine trade-offs between high vacuum gas oil (HVGO) yield and total annualised cost (TAC) of a refinery that considers the needs of downstream operations. In this work, crude oil blending ratio, furnace outlet temperature, flash zone temperature, column top pressure, column bottom pressure, stripping steam flowrate, HVGO pump-around flowrate, and light vacuum gas oil (LVGO) pump-around flowrate of the VDU are to be optimised. Based on the optimised result, the heavy-light crude blend achieves higher HVGO yield and lower TAC, and the optimised results were validated with the simulation results via Aspen HYSYS. The proposed methodology was proven to have accurate estimations of the VDU operation in the process simulation environment. Moreover, the optimised results can provide insight into the optimal process conditions of VDU for the refiners. With this insight, effective operating strategies can be developed to overcome the limitations present in real VDU operations.

Keywords Vacuum distillation unit (VDU) · Surrogate modelling · Process simulation · Heavy vacuum gas oil · Process optimisation

Introduction

Crude oil is a petroleum product composed of hundreds of hydrocarbons with water, nitrogen, sulphur, salts, nitrogen-containing compounds, and some metal complexes (Mittal et al. 2011). In the petroleum refining industries, the crude distillation unit is the first processing unit in all petroleum refineries. Such unit is the most important unit to break and separate crude oil into simpler and useful mixtures. However, the crude distillation unit is energy-intensive as it uses up the fuel at the equivalent of 1–2% of the processed crude oil in a refinery. Thus, such unit has the highest operating costs in a refinery (Gu et al. 2014). Therefore, the retrofit and optimisation of crude distillation units received considerable research interest to improve the economic performance of a refinery.

✉ Viknesh Andiappan
vmurugappan@swinburne.edu.my

1 School of Engineering and Physical Sciences, Heriot-Watt University Malaysia, 62200 Putrajaya, Wilayah Persekutuan Putrajaya, Malaysia

2 School of Engineering and Technology, Sunway University, Jalan Universiti, No. 5, Bandar Sunway, 47500 Petaling Jaya, Selangor Darul Ehsan, Malaysia

3 Safety and Health Research Group, Universiti Teknologi Malaysia, 81310 UTM Johor Bahru, Malaysia

4 Biomass Waste-to-Wealth Special Interest Group, Research Centre for Sustainable Technologies, Faculty of Engineering, Computing and Science, Swinburne University of Technology Sarawak Campus, Jalan Simpang Tiga, 93350 Kuching, Sarawak, Malaysia

Figure 1 shows a typical process flow diagram of a typical crude distillation unit, processing crude oil. Such unit consists of a pre-flash unit, an atmospheric distillation unit, and a vacuum distillation unit (VDU). VDU is part of a typical refinery process that helps to further recover the higher boiling gas oil from the atmospheric residue of an atmospheric distillation unit. As its name implies, VDU operates under vacuum conditions (i.e. below atmospheric pressure). At such low pressure, the boiling point of the feed of VDU is low enough to break down the products without cracking or degrading the crude oil (Treese et al. 2020). The major products of the VDU include light vacuum gas oil (LVGO) and heavy vacuum gas oil (HVGO). In VDU, separating atmospheric residue into products involves complex relationships between input and output variables. The input variables refer to the feedstock properties and the operating conditions of the VDU. Meanwhile, the output variables of VDU are product flowrate, product quality, and plant profit. However, it is challenging to define and maintain an optimal operating condition owing to the complex relationships between the input and output variables of VDU (Liau et al. 2004).

In the last decade, the diversification of crude slate and fluctuations in crude oil prices have pushed refiners to seek opportunities to produce mixtures of crude oils (Huang et al. 2017). To accommodate such variation in crude oil properties, the operating conditions of VDU need to be adjusted from time to time to ensure product quality and reduce the disruption to the downstream processes. Note that such adjustments will consequently impact the product yield and quality. This is critical because the products of VDU serve as the feedstock to the downstream process units, such as hydrocrackers, fluid catalytic crackers, or lube oil facilities (Martin and Nigg 2001). If the product yield or product quality specifications cannot meet downstream requirements, the refinery will experience output disruptions. Such incidents may also cause an unplanned shutdown of the units and eventually incur a financial loss in the refinery. Hence, these consequences raise the need to develop a systematic optimisation method for determining the blending ratio of different kinds of crude oil and the optimal operating conditions of the VDU. With such method, the operation of VDU can maintain high production throughput and satisfactory product quality and sustain the economic performance of the refinery. In the past, several studies have been performed to optimise distillation systems. The following sub-sections discuss the methods used in these studies, highlight the gaps in research, and present the novelty of this work.

Literature Review

Mathematical Programming in Distillation Systems

Mathematical programming has been widely applied to optimise crude distillation units (Pintarič and Kravanja 2006; Seo et al. 2000; Basak et al. 2002; Gu et al. 2015; Inamdar et al. 2004; Al-mayyahi et al. 2011; Foo et al. 2017; More

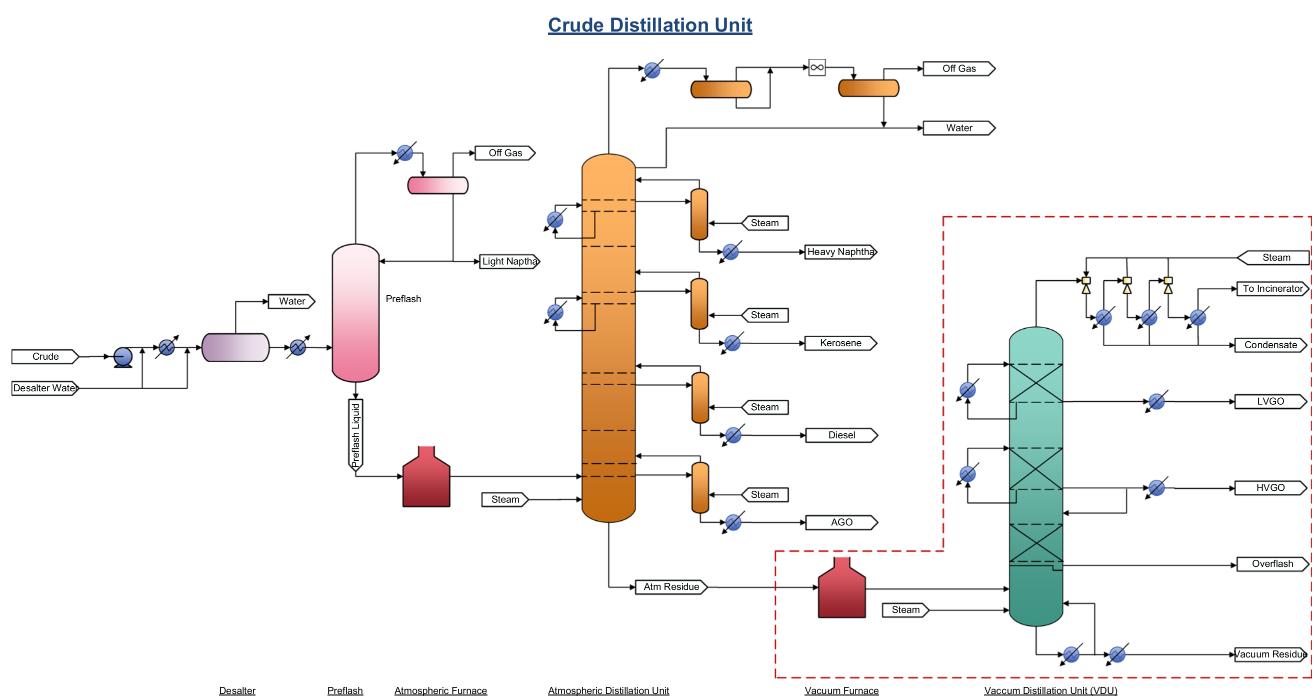

Fig. 1 Process flow diagram of a typical crude distillation unit

et al. 2010). Past studies have used mathematical programming to determine the optimal solutions for distillation systems expressed and modelled as mathematical Eqs. 7. For instance, Seo et al. (2000) developed mixed-integer nonlinear programming model to determine crude distillation unit's optimal feed location and operating conditions. With that, the proposed framework reduced the operating and capital costs of the existing crude distillation unit by 86%. Next, a nonlinear, steady-state crude distillation unit was developed by Basak et al. (2002) to maximise the net profit while satisfying the product properties. Gu et al. (2015) combined exergy analysis and mathematical programming for the energy optimisation of the multi-stage crude oil distillation units, which were able to reduce 2.79% in energy consumption. However, distillation units have multiple criteria and requirements that need to be addressed simultaneously.

In response to this, multi-objective models were developed. For example, Inamdar et al. (2004) introduced elitist nondominated sorting genetic algorithms to address the multi-objective optimisation of the crude distillation systems. Besides, Huang et al. (2017) employed a multi-objective optimisation model to investigate the trade-off between economic benefit, furnace energy consumption, and carbon dioxide (CO_2) emissions of the crude distillation unit. Meanwhile, the effect of binary feed composition on the crude distillation unit has also been investigated. The proposed model provided a set of Pareto-optimal solutions that can resolve the limitations of the refinery. Similarly, a multiple-objective optimisation approach was developed by Al-Mayyahi et al. (2011) to determine the trade-off between the CO_2 emissions and operating revenue for different crude blends in the crude distillation systems.

Process Simulation in Distillation Systems

On the other hand, several studies have implemented the use of established process simulation packages to simulate distillation systems. Process simulation packages are software capable of designing an operational model for a given process and that model is used to predict how that process will behave under certain operating conditions (Foo et al. 2017). Examples of these packages may include (but are not limited to) Aspen HYSYS, Aspen Plus, Unisim, and PRO II. More et al. (2010) developed a simulation model for a crude distillation unit via Aspen Plus to investigate the impact of feed composition with the objective function of maximising the net profit. As reported in More et al. (2010), process simulation via Aspen Plus is not a correct approach to optimise the continuous and binary variables, including feed location and side stream location, in the crude distillation unit. Meanwhile, Ibrahim et al. (2017a) applied a simulation-optimisation approach simultaneously to design a single-stage crude distillation system and heat recovery network. This approach overcame the complex interactions between the units in the crude distillation system. Based on the abovementioned literature, some researchers have applied mathematical programming techniques to optimise crude distillation units. Nevertheless, the complexity and nonlinearities associated with the distillation units may restrict the use of the mathematical optimisation model. To overcome the above limitation, researchers explored surrogate modelling techniques in distillation optimisation, particularly for the crude distillation units in a refinery.

Surrogate Modelling in Distillation Systems

A surrogate model is a sophisticated analytic model that mimics the complex behaviour of the simulation environment based on the regression of statistical input variables and output responses (Loper 2015; Denimal et al. 2016). This allows surrogate models to mimic distillation systems in a simple and fairly accurate manner. Surrogate modelling techniques are employed to capture the relationship between the independent X variables and dependent Y variables of the distillation system. The independent X variables refer to the variables that can be controlled (i.e. crude oil blending ratio and operational variables), whereas dependent Y variables are the variables that are measured and dependent on the independent variables (i.e. HVGO yield, pump-around cooler flowrate, column diameter). A surrogate model is constructed by regressing against a set of statistical data. The data is later converted to a fairly representative equation that can describe the operation of the distillation system.

López et al. (2009) proposed a nonlinear programming algorithm optimisation model with the surrogate modelling technique to optimise the crude distillation unit. The proposed model maximised the crude distillation system profits and determined the optimal operating conditions for each atmospheric column. It is worth noting that López et al. (2013) then implemented surrogate models in a nonlinear programming model to investigate the effect of crude composition and operating conditions of the crude distillation unit. With the optimisation objective function as maximising the economic potential, an increase of 13% in profit was observed. Besides, Yao and Chu (2012) developed a surrogate model with support vector regression and improved the design of the experiment method to optimise the operating conditions of the atmospheric distillation unit. An increase in profitability was reported in the proposed approach. Apart from that, a cut-point temperature surrogate modelling technique was proposed by Gut et al. (2020) to determine the product yield and properties of the crude distillation units. Surrogate modelling has been applied in other areas, such as acid gas removal systems (Chew et al. 2022) and free fatty acid removal deodorizers (Tan et al. 2021). Surrogate models were proven to have accurate estimations.

Metaheuristic Optimisation in Distillation Systems

Other than mathematical and surrogate modelling, various metaheuristic optimisation methods were also applied in optimising the performance of distillation systems. Liau et al. (2004) and Motlaghi et al. (2008) developed an artificial neural network (ANN) model to predict the crude oil distillation units' operating conditions and product quality. Liau et al. (2004) used their ANN model to maximise the oil production rate. Motlaghi et al. (2008) did the same but extended that to minimise the model output error. Nevertheless, these approaches offered online optimisation results related to the crude oil properties of the refiners. Moreover, Ochoa-Estopier et al. (2013) introduced an ANN model to represent distillation columns. The proposed model included heat exchanger networks into the optimisation framework to determine the optimal operating conditions that give maximum process economy. After that, Ochoa-Estopier and Jobson (2015) implemented the ANN to maximise the production throughput while simultaneously maximising the net profit of the heat-integrated crude oil distillation units. Additionally, Ochoa-Estopier et al. (2018) extended their work to determine the factors influencing product yields and energy consumption in the crude distillation unit. The results demonstrated a significant profitability increase of $7.2 million annually. Moreover, a bootstrap aggregated neural network was employed by Osuolale and Zhang (2016) to enhance the reliability and accuracy of the ANNs model. This model was used to determine the optimal operating conditions of the distillation columns that maximise exergy efficiency while satisfying the product quality specifications. As reported in Osuolale and Zhang (2016), there is a 32.4% improvement in exergy efficiency. Ibrahim et al. (2017b) introduced the combination of the ANN and support vector machine to optimise the crude distillation units' column configurations and operating conditions. Furthermore, Ibrahim et al. (2020) also implemented the ANN with the support vector machine technique to design heat-integrated crude oil distillation units. This proposed model could simultaneously process multiple crude feeds and maximise the economic potential.

Optimisation Studies on Vacuum Distillation Units (VDUs)

Past studies have implemented various methods to optimise distillation systems, with crude distillation systems and atmospheric distillation units being the central focus. As mentioned previously, the performance of VDU is significant as it needs to satisfy the feedstock quality and rate target of the downstream process units. Therefore, a small number of researchers have focused on optimising VDUs. With the aid of Aspen HYSYS simulation, Mittal et al. (2011) developed an optimisation framework for crude oil blending and processing with the simultaneous considerations of the furnace energy consumption, CO_2 emissions, and economic potential of the VDU. Next, Gu et al. (2014) proposed a methodology to analyse and evaluate three crude oil vacuum distillation processes. The proposed methodology also considered recovery energy and exergy efficiencies, economic potential, and product yield. Consequently, the results provided insight for engineers to determine a suitable process and outlet temperature for the VDU. Interestingly, (Li et al. 2017) introduced a dividing wall column in a lubricant-type VDU to enhance the product yield and quality. The proposed configuration showed that the lube cut's boiling point range was reduced significantly, improving the product yield and quality.

Research Gaps

Several critical observations can be noted from the literature review above:

- Firstly, previous studies that have considered optimisation, simulation, and surrogate modelling in distillation focus primarily on the crude distillation units (CDUs). The operation of VDUs is complex as its total annualised cost (TAC) can be influenced by multiple operating parameters. In addition, many of the operating parameters affect TAC in a nonlinear manner. This makes it challenging to model VDU operations accurately, especially based on operating conditions, crude blending composition, and HVGO yield. Less attention was given to optimising the total annualised cost (TAC) in vacuum distillation units (VDUs) based on crude blending composition, operating conditions, and HVGO yield.
- Aside from this, the relationship between the product yield and TAC of VDU has not been studied for crude oil blending. When product yield is prioritised, the TAC of the VDU might be very high. On the other hand, if TAC is the main focus, the product yield will be compromised. Hence, a trade-off between product yield and TAC is required. Furthermore, refiners have been looking for the opportunity to process lower-cost heavy crude oil due to operational and feed availability constraints. By blending the crude oil, the diversity of crude oil processing as feedstock has increased, which maximises refiners' profitability. Therefore, crude oil blending must be considered in the optimisation of VDUs.
- Another observation that can be drawn from the literature cited above is that no work has combined process simulation tools, surrogate modelling, and mathematical programming for VDU optimisation. Process simulation tools simulate and provide basic data on distillation sys-

tems. Nevertheless, many challenges occur in the optimisation process using process simulation tools due to the high degree of freedom and nonlinearities associated with the distillation units. As mentioned, a trade-off between HVGO yield and TAC is required; however, the process simulation tool cannot perform multi-objective optimisation. This is because the simulation tool cannot optimise several variables in one run and perform operational pathway selection. Furthermore, the process simulation tool does not reflect the optimal solution to run a system. It can only give the best possible solution based on the decision-makers' pre-defined scenarios. (Lee 2017)

Contribution of This Work

To address the gaps described previously, this work presents a multi-objective optimisation methodology combining strengths from process simulation, surrogate modelling, and mathematical programming. The surrogate model is constructed by regressing against a set of statistical data generated from process simulation of a VDU. The data is later converted to a fairly representative equation that can describe the operation of the VDU. Mathematical programming is then used to analyse and provide the optimal solution for the VDU. Therefore, combining the individual strengths of these three methods can reveal results that cannot be determined when these methods are used separately. Combining these methods is essential for decreasing the overall process costs, predicting the process behaviour, improving the utilisation of resources, and providing detailed information on how the system operates.

Moreover, the proposed methodology is used to investigate the impact of crude blending composition and the operating conditions of the VDU on the HVGO yield. Besides, upon considering the economic profit of refineries, the TAC of VDU is further investigated. This study can provide economic and operational benefits to the refiners as it can overcome the fluctuation of crude oil prices and tighter supply–demand constraints in the refinery. The objectives of this research are as follows:

- To determine the optimal VDU operating performance and conditions with maximum HVGO
- To determine the optimal VDU operating performance and conditions with minimum TAC

The remainder of this paper is organised as follows. The 'Methodology' section presents the methodology for optimising VDU based on process simulation, surrogate modelling, and mathematical programming. The 'Case Study' section illustrates the application of the proposed methodology in a case study. In the case study, different crude blending ratios are compared and analysed to identify the optimal crude blending ratio with the corresponding operating conditions that give maximum HVGO yield and minimum TAC. The 'Results and Discussion' section presents the optimised results with the corresponding crude blending ratio and operating conditions. The optimised results are then tested in the simulation model, and a comparison between these two sets of results is discussed. Finally, the conclusion and future work are given in the 'Conclusion and Future Work' section.

Methodology

Figure 2 shows the research methodology of this work. The work can be divided into three primary stages: process simulation, surrogate modelling, and mathematical optimisation.

Referring to Fig. 2, after data collection, Stage 1 of the methodology includes crude oil characterisation, crude oil blending model, and modelling of rigorous vacuum distillation. The process information of the VDU is generated after running the simulation model with different crude oil compositions and operating conditions. The generated process information is used in Stage 2 of the methodology, where VDU surrogate models are constructed. The surrogate models are used to capture the relationship between the selected input and output variables for the complex VDU operation. In this work, two input variables related to crude oil ratio and VDU operating conditions and four output variables (i.e. HVGO yield, column diameter, HVGO pump-around cooler flowrate, and LVGO pump-around cooler flowrate) are chosen for the development of surrogate models. These variables were chosen as they were identified as key elements that influence heavy vacuum gas oil (HVGO) yield and total annualised cost (TAC) of the VDU. By performing the validation via statistical analysis, the input variables that significantly impact the output variables are included in the development of surrogate models. In Stage 3, an optimisation model is developed to determine the optimum operation conditions based on the objectives, as discussed in the 'Contribution of This Work' section. However, HVGO yield and TAC of VDU are conflicting targets. For instance, when HVGO yield is increased, the TAC will also increase. This is undesirable as low TAC would be preferred. Therefore, a trade-off between HVGO yield and TAC of the VDU is required. The implementation of the multi-objective optimisation model addresses this. To ensure the validity of the optimisation model, the optimal results (i.e. operating conditions) from the model are updated into the process simulation model. If the updated conditions in the simulation do not provide comparable results, the first step, i.e. data collection, will be revisited. Here, the data used as constraints for the

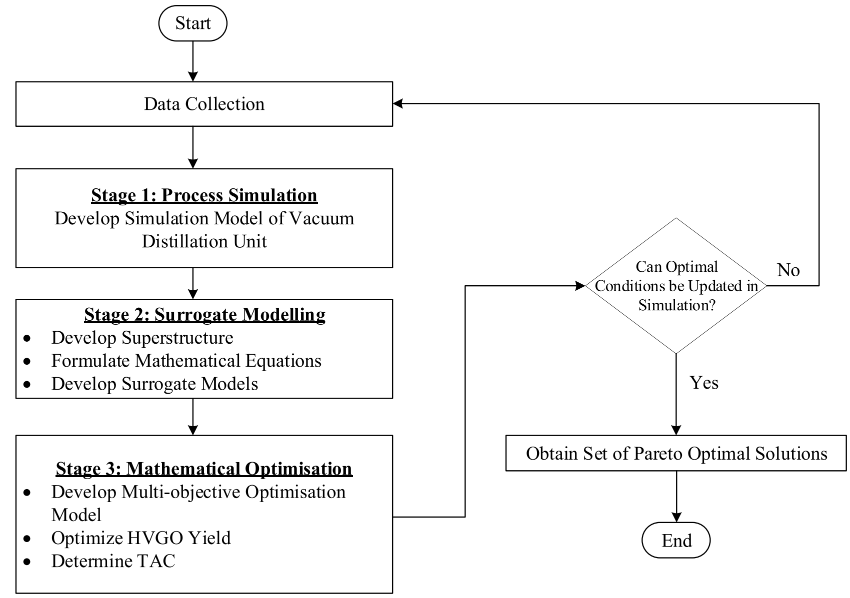

Fig. 2 Overview of methodology

process simulation will be checked. If this step is considered satisfactory, the following steps will be revisited for further checking and updates. Finally, the Pareto-optimal solutions are obtained from the optimisation model, which can be used to develop physical insight for the decision-makers in determining a preferred solution. The above description provides a conceptual framework of VDU optimisation, as illustrated in Fig. 3. The following sub-sections will provide clear details of the three previously mentioned stages.

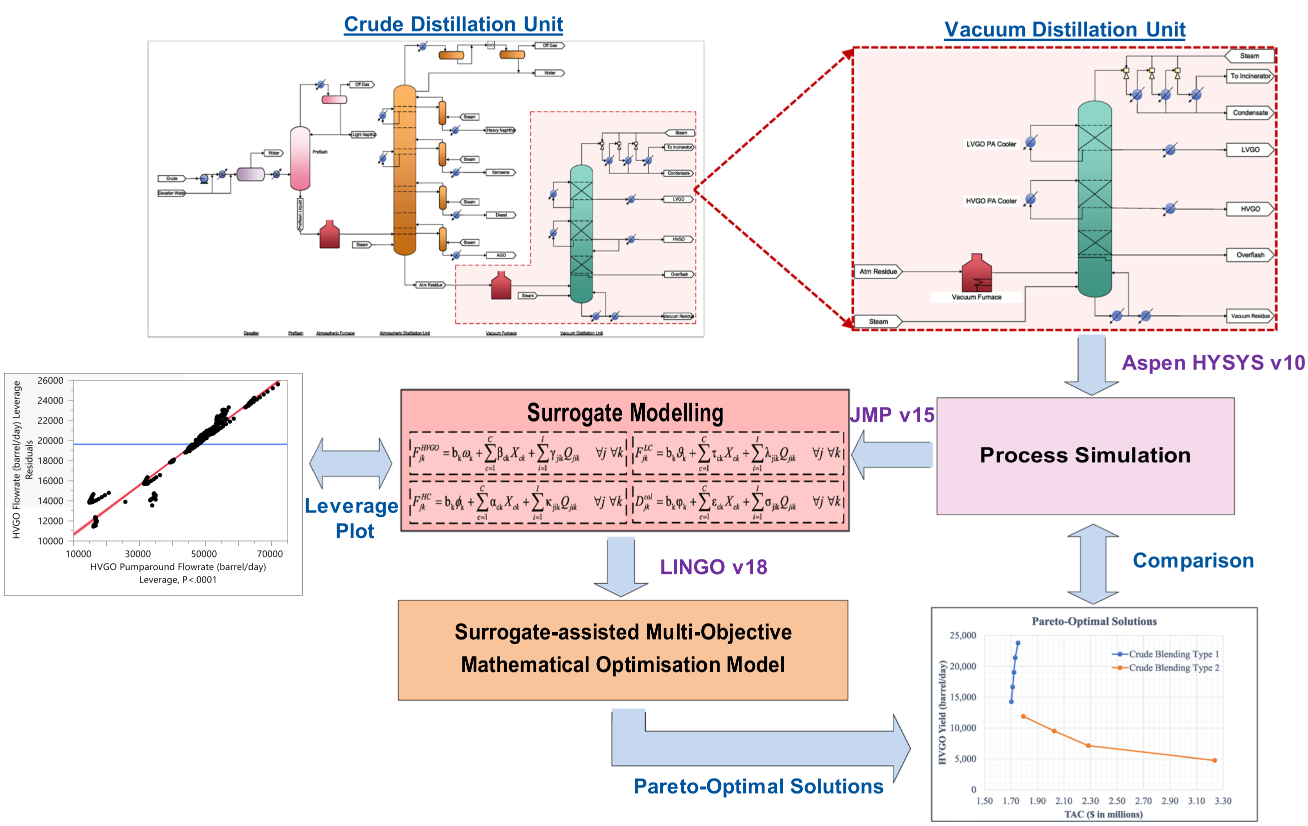

Fig. 3 Conceptual framework for optimisation of the vacuum distillation unit (VDU)

Stage 1: Process Simulation

Generally, two types of models can be used to design the crude distillation unit: the shortcut model and the rigorous model. A rigorous model can simulate mass balance, energy balance, and equilibrium relations for every stage of the distillation unit. Therefore, the rigorous model is chosen in this research study as it provides more accurate predictions. Commercial process simulation software (i.e. Aspen HYSYS, Aspen Plus, PRO/II of SimSci-Esscor) is commonly used for modelling crude distillation units in the refinery. In this work, Aspen HYSYS version 10.0 is selected to develop the crude oil blending and rigorous distillation models of the VDU. This is because Aspen HYSYS contains existing routines specific to solving the distillation columns, unlike other software.

Crude Oil Characterisation and Blending

This work considers three crude assays as different choices of crude blends. Heavy crude is considered one of the crude assays. Meanwhile, higher API gravity crude assays, namely light and medium assays, are considered for the remaining crudes. As mentioned in the previous section, crude oil blending plays an important role in maximising the refinery's profitability. Therefore, a crude oil blending model is considered to mix the heavy crude with other crudes to be processed as feedstock in the distillation operation. To do this, the assay data of the crude oil is first added to Aspen HYSYS to generate the working curves, such as internal true boiling point, molecular weight, density, and viscosity curves. Then, a set of hypothetical pseudo-components representing each crude oil is created from the working curves. By using the oil product cut option, different types of crude oil are blended in a designated ratio in the oil environment of Aspen HYSYS. Once the blending is completed, the crude oil is installed in the simulation environment, and the rigorous distillation model of the crude distillation unit is built and discussed in the 'Simulation Development' section.

Simulation Development

The crude distillation unit is simulated based on the operating parameters and column specifications listed in Aspen HYSYS version 10, which has been validated (Aspen 2017). To perform a reliable simulation model, an appropriate thermodynamic fluid package is determined based on the composition of the selected crude oil. The simulation model of the crude distillation unit included preheating trains, an atmospheric distillation unit, and VDU, as shown in Fig. 4.

In this work, the atmospheric distillation unit consisted of 50 trays, one total condenser, three side strippers, and three pump-arounds. The products of the atmospheric distillation unit are naphtha, kerosene, diesel, atmospheric gas oil, and atmospheric residue. Meanwhile, the atmospheric distillation unit's atmospheric residue is fed into VDU, consisting of 14 trays and two pump-arounds. After that, VDU allowed fractionation of the atmospheric residue into off-gas, light vacuum gas oil, heavy vacuum gas oil, slop wax, and vacuum residue under vacuum pressure. The process information of VDU is generated after running different types of crude blends in the constructed simulation model.

It is worth noting that the number of stages for the distillation columns was determined using a series of procedures. The procedures consist of various levels of simulation rigour. Firstly, a component splitter was used to determine the separation ratios and operating conditions required to achieve the required yield. With the removal ratios and operating conditions, a shortcut distillation simulation was performed to determine the number of stages required to achieve the said yield. The number of stages here is then used as input data for the rigorous simulation model to establish the baseline performance of the distillation column. This baseline simulation model is later used to develop sampling points for the regression analysis. Thus, the number of stages in the column is assumed to be fixed. The goal is to evaluate how the operating conditions and yield would impact the column cost (i.e. column

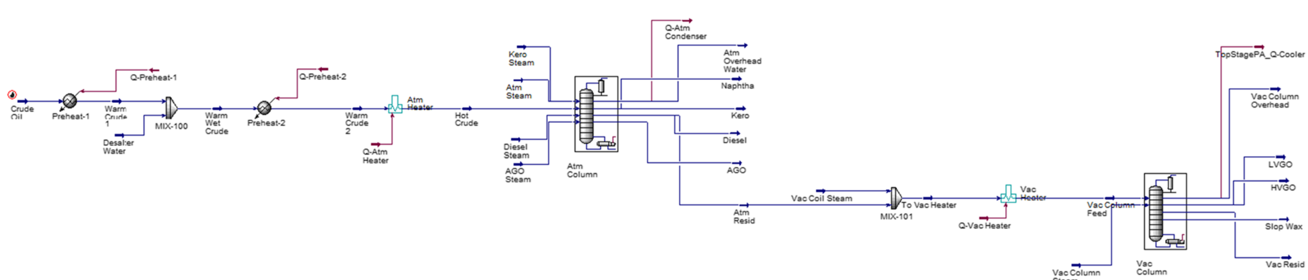

Fig. 4 Aspen HYSYS simulation layout of the vacuum distillation unit

diameter, column height, wall thickness, material construction, installation cost factor). Due to this assumption, the results of this presented work would not rely on the number of stages. It is also important to add that the scope of this study does not perform simulation verification with real plant data. This can be identified as a limitation of this study and serve as a basis for further improvement.

Stage 2: Surrogate Modelling

In the second stage, the surrogate modelling technique is employed to represent the simulation environment of the VDU. The surrogate model is built around the data generated from the simulation model developed in the 'Stage 1: Process Simulation' section with a random selection of input variables and their corresponding bound limits. The sampling points are generated by varying the operating parameters for the VDU simulation and subsequently noting down the outputs. For instance, the pressure is varied between a range of values, to determine the corresponding values for stripping steam flowrate, HVGO pump-around flowrate, etc. The data is then regressed and converted into equations that can be used to represent the operation of the distillation system. One advantage of the surrogate model is that it allows a rapid calculation of the model output responses by applying equations to relate the input variables to the output responses. Two types of surrogate models have been reported in many publications: polynomial response surface equations and ANNs. Compared to the response surface method, an ANN in the distillation column is more complicated, consists of more intensive steps, and requires more investigation for the data regression (Ibrahim et al. 2017a). On the other hand, the major advantage of the polynomial response surface equation is that it requires a very short computational time to study the relationship between the factors. The behaviour between the output responses and the important influencing variables can be captured easily using regression analysis (Aydar 2018). Besides, the response surface method can produce a mathematical expression based on the data supplied, which can be used mathematically to represent the system's performance. The aforementioned mathematical expression can be integrated into a mathematical optimisation model to enhance and optimise a process or a system. The integrated expression can be used in a mathematical model to obtain optimal responses with minimum variance and a small number of controlled parameters. Such integration allows the decision-makers to make more informed decisions about the system's operation. Hence, the polynomial response surface equation is selected to be used in this work. A general first-order polynomial function of a response surface equation is expressed in the following form:

$$Y = \mathrm{z} + \sum_{n=1}^{N} \beta_n X_n \tag{1}$$

where Y represents the dependent variables, X represents the independent variables, z is the intercept regression coefficient, β_n is the linear term regression coefficient, and N is the number of factors.

Due to the complexity and nonlinearity of VDU operations, the surrogate modelling technique is applied in this work to represent the relationship between the input and output responses. The surrogate models of VDU are built based on the aforementioned polynomial response surface equation. Before constructing VDU surrogate models, the dependent and independent variables are determined. In order to achieve the objectives of this research study, four dependent variables, such as HVGO yield, HVGO pump-around cooler utility flowrate, LVGO pump-around cooler utility flowrate, and column diameter, are considered. Meanwhile, the crude oil blending ratio and operating conditions of VDU are selected as the independent variables for all the dependent variables.

Besides, a superstructure is built before the development of the surrogate model. A superstructure is a schematic diagram representing all of a system's possible routes. With the aid of the superstructure, all the possible operating routes and their respective interconnections to obtain the output responses of the VDU are determined. In this work, the operating routes represented different crude oil blending ratios and operating conditions in the VDU, as illustrated in Fig. 5.

As shown, each crude oil stream, c(i.e. heavy, medium, light), with a different crude oil blending ratio, X_{ck}, is introduced into the crude oil blending model, k(i.e. heavy-medium, medium-light). Then, the crude oil blending model combines different crude oil streams in a designated ratio. After blending, each crude blend is fed into the VDU separately to perform fractionation. The VDU's operating conditions vary according to the crude blend composition. As a result, different output variables values are obtained and used for the development of the surrogate model. In order to represent the crude oil blending model shown in Fig. 2, crude oil mass flow calculations are carried out as follows:

$$F_c^{\mathrm{av}} \geq F_c \; \forall c \tag{2}$$

$$F_{ck} = F_c X_{ck} \; \forall c \, \forall k \tag{3}$$

$$\sum_{c=1}^{C} F_{ck} = F_k^{\mathrm{Tot}} \; \forall k \tag{4}$$

where F_c^{av} represents the availability of crude feed and F_c is the mass flow crude utilised. Note that F_c is bounded by the available amount of crude feed F_c^{av}. F_{ck} indicates the mass flowrate of the crude oil with a certain blend ratio, X_{ck}, that

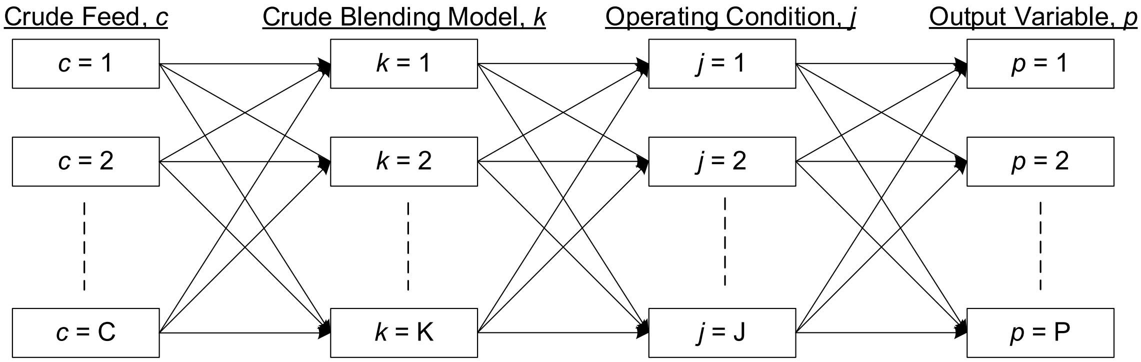

Fig. 5 Generic superstructure of vacuum distillation unit in the surrogate model development

feeds into the crude oil blending model, while F_k^{Tot} is the total crude flowrate of particular blend (i.e. heavy-medium, medium-light).

After the development of the superstructure, the surrogate model is constructed to capture the relationship between the selected independent variables and dependent variables. Each model is a function of the independent variables of crude oil blending ratio and operating conditions with its respective dependent variable. The polynomial response surface equations of each surrogate model are expressed below, which will use the same form as in Eq. (1):

$$F_{jk}^{\mathrm{HVGO}} = b_k\omega_k + \sum_{c=1}^{C}\beta_{ck}X_{ck} + \sum_{i=1}^{I}\gamma_{jik}Q_{jik}\,\forall j\,\forall k \tag{5}$$

$$F_{jk}^{\mathrm{HC}} = b_k\phi_k + \sum_{c=1}^{C}\alpha_{ck}X_{ck} + \sum_{i=1}^{I}\kappa_{jik}Q_{jik}\,\forall j\,\forall k \tag{6}$$

$$F_{jk}^{\mathrm{LC}} = b_k\vartheta_k + \sum_{c=1}^{C}\tau_{ck}X_{ck} + \sum_{i=1}^{I}\lambda_{jik}Q_{jik}\,\forall j\,\forall k \tag{7}$$

$$D_{jk}^{\mathrm{col}} = b_k\varphi_{\mathrm{k}} + \textstyle\sum_{c=1}^{C}\varepsilon_{ck}X_{ck} + \sum_{i=1}^{I}\sigma_{jik}Q_{jik}\ \ \forall j\forall k \tag{8}$$

$$b_k \in \{0, 1\}$$

where F_{jk}^{HVGO} is HVGO yield, F_{jk}^{HC} is HVGO pump-around cooler utility flowrate, F_{jk}^{LC} is LVGO pump-around cooler utility flowrate, and D_{jk}^{col} is the column diameter. Besides, X_{ck} indicates the crude oil blending ratio, as evaluated in Eqs. (2–4). Q_{jik} indicates a set of operating conditions, j, that vary based on the crude blend, k. Moreover, i represents each operating condition in the particular set of operating conditions such as column temperature, column pressure, stripping steam flowrate, and pump-around flowrate $\beta_{ck}, \alpha_{ck}, \tau_{ck}, \varepsilon_{ck}$ are the linear term regression coefficients with respect to X_{ck}, whereas $\gamma_{jik}, \kappa_{jik}, \lambda_{jik}, \sigma_{jik}$ are the linear term regression coefficients with respect to Q_{jik}. $\omega_k, \phi_k, \vartheta_k, \varphi_k$ are the intercept regression coefficients of each polynomial response surface equations. Furthermore, the binary variable b_k is introduced in the equations where the values 0 and 1 are used to signify the activation or deactivation of the parameters in the particular surrogate model. All the polynomial response surface equations from Eqs. (5)–(8) are subjected to the bound limits as described below:

$$b_kX_{ck}^{\mathrm{L}} \le X_{ck} \le b_kX_{ck}^{\mathrm{U}}\,\forall c\,\forall k \tag{9}$$

$$b_kQ_{jik}^{\mathrm{L}} \le Q_{jik} \le b_kQ_{jik}^{\mathrm{U}}\,\forall j\,\forall i\,\forall k \tag{10}$$

where L and U superscripts represent the lower and upper bounds of the independent variables, X_{ck} and Q_{jik}, respectively. The bound limits of each independent variable are further discussed in the ‘Case Study’ section.

In order to determine the coefficient values that make up the response surface equations above, a large number of sample points are generated from the simulation model developed in the previous stage. The number of sample points is determined based on the amount of data available for the equipment considered, the amount of data available after data pre-processing, and the quality of the regressions generated using the available data. In this work, the sample points are generated by varying the crude oil blending ratio and operating conditions of VDU. Statistical analysis software (i.e. JMP, Python) is typically used to regress the generated sample points in response surface equations (Loper 2015). In this work, JMP version 15.0 is selected to regress the response surface equations because it can easily assess the data from various sources, allowing users to build their model rapidly. Besides, JMP can link the statistical data to interactive graphics, which helps the user to explore and visualise their data better. After the regression analysis, validation analysis is carried out to evaluate the accuracy of surrogate models. An evaluation of *R*-square, *P*-value, and leverage plots is considered. The *R*-square of the equations must be greater than 0.90 to indicate a good fit of data, while the *P*-value of each variable must be smaller than 0.05 to show a significant impact on the dependent variable. The impacts of each independent variable on the dependent variables are further identified using the leverage plots. By performing the validation analysis, those independent variables that have a weak impact on the dependent variables are excluded from the development of the surrogate models. However, it is important to highlight that these models come with a certain confidence level. The confidence level of these models can be improved through enhancing data sample size and performing data cleaning. Finally, the surrogate models are built and implemented in the optimisation model, as discussed in the 'Stage 3: Mathematical Optimisation' section.

Stage 3: Mathematical Optimisation

Many mathematical programming tools are available to develop the distillation optimisation model. In this work, a commercial optimisation software, LINGO version 18.0 is used to develop an optimisation model to maximise the HVGO yield with the simultaneous consideration of minimising the TAC of the VDU. However, these two objectives are contradicting in nature. Therefore, multi-objective optimisation is implemented in this work to trade off between two conflicting objectives simultaneously. The multi-objective optimisation model is developed based on the polynomial response surface equations of the surrogate models and the superstructure, as discussed in the 'Process Simulation in Distillation Systems' section. The overall optimisation model includes an objective function, decision variables, and constraints. In this work, two optimisation objective functions of maximising HVGO yield and minimising TAC are investigated simultaneously. The procedures for estimating these objectives are evaluated in the 'Total Annualised Cost (TAC)' section and 'Heavy Vacuum Gas Oil (HVGO) Yield' section, respectively. On the other hand, the model's constraints are in the form of equality and inequality expressions. Meanwhile, the decision variables considered in this work are crude blending ratio, furnace outlet temperature, flash zone temperature, top column pressure, column bottom pressure, stripping steam flowrate, HVGO pump-around flowrate, and LVGO pump-around flowrate. These variables are varied to achieve an optimal value for the objective functions. With the aid of the multi-objective optimisation model, a set of Pareto-optimal solutions with a different trade-off between HVGO yield and TAC is determined. A Pareto-optimal solution is a set of nondominated solutions which means an improvement in one objective without losing in another objective is not possible (Andiappan 2017). With these Pareto-optimal solutions, a greater insight into the optimal process condition of the VDU can be provided to the refiners.

Total Annualised Cost (TAC)

The objective function of minimising TAC is shown below:

$$\text{Minimise}\,TAC \tag{11}$$

where

$$TAC = \text{ACC} + \text{OC} \tag{12}$$

TAC of the vacuum distillation unit is the sum of the annualised capital cost (ACC) and operating cost (OC). The annualised capital cost is the summation of the installed cost of column shell (S^C) and the installed cost of the trays within the distillation column (T^C), with the multiplication of the annualised capital factor (C^{rf}). The annualised capital cost is expressed as below:

$$\text{ACC} = (S^C + T^C) \times \text{C}^{\mathrm{rf}} \tag{13}$$

$$C^{\mathrm{rf}} = \frac{r(1+r)^t}{(1+r)^t - 1} \tag{14}$$

where t is the technology life span and r is the interest rate of the return. In this work, the technology life span is set as 20 years and the interest rate of return is assumed to be 10%.

The installed cost of column shell and installed cost of trays within the column are calculated using the following correlations, proposed by Towler and Sinnott (Andiappan 2017):

$$S^C = \sum_{j=1}^{J} \sum_{k=1}^{K} S^C_{jk} \tag{15}$$

where

$$S^C_{jk} = \left[a^{\mathrm{s}} + b^{\mathrm{s}} \left(\pi \times D^{\mathrm{col}}_{jk} \times H \times t^{\mathrm{w}}_{jk} \times \rho\right)^{n^{\mathrm{s}}}\right] \times F^{\mathrm{s}}\, \forall j\, \forall k \tag{16}$$

$$T^C = \sum_{j=1}^{J} \sum_{k=1}^{K} T^C_{jk} \tag{17}$$

where

$$T^C_{jk} = \left[a^{\mathrm{t}} + b^{\mathrm{t}} (D^{\mathrm{col}}_{jk})^{n^{\mathrm{t}}}\right] \times N^{\mathrm{t}} \times F^{\mathrm{t}}\, \forall j\, \forall k \tag{18}$$

In the above equations, a^{s} and b^{s} and a^{t} and b^{t} are the cost coefficients of column shell and tray, respectively; n^{s} and n^{t} are the exponent of column shell and tray, respectively; D^{col}_{jk} is the column diameter; H is the column height; t^{w}_{jk} is the wall thickness; ρ is the density of material construction; N^{t} is the total

Table 1 Fixed parameters used in installed cost calculation of column shell

Parameters	Values	Parameters	Values
a^s	17,000	H (m)	40
b^s	79	$\rho(\mathrm{kg/m^3})$	8000
n^s	0.85	F^s	4

Table 2 Fixed parameters used in installed cost calculation of trays

Parameters	Values	Parameters	Values
a^t	130	N^t	14
b^t	440	F^t	1.3
n^t	1.8		

number of trays of vacuum distillation unit; F^s is the column shell installation factor; and F^t is the tray material cost factor.

D_{jk}^{col} is determined using the polynomial response surface equation of the surrogate model, as stated in Eq. (8). Meanwhile, t_{jk}^{w} can be calculated using a lot of well-published methods, which is further discussed in the 'Case Study' section. The values of other fixed parameters are summarised in Tables 1 and 2.

Furthermore, the calculation of the operating costs only considered the utility cost of pump-around coolers and other stream costs that will affect the operating condition of VDU. Other operating costs such as crude oil prices, labour cost, and transportation cost are not included. The operating cost of VDU is calculated using the equation as shown below:

$$\mathrm{OC} = \sum_{j=1}^{J}\sum_{k=1}^{K} F_{jk}^{\mathrm{HC}} C_{jk}^{\mathrm{HC}} + \sum_{j=1}^{J}\sum_{k=1}^{K} F_{jk}^{\mathrm{LC}} C_{jk}^{\mathrm{LC}} + \sum_{j=1}^{J}\sum_{i=1}^{I}\sum_{k=1}^{K} Q_{jik} C_{jik} \tag{19}$$

where F_{jk}^{HC} and C_{jk}^{HC} are the utility flowrate and utility cost of HVGO pump-around cooler, respectively; F_{jk}^{LC} and C_{jk}^{LC} are the utility flowrate and utility cost of LVGO pump-around cooler, respectively; $Q_{jik}C_{jik}$ are the cost of other important streams which are further determined in the 'Optimisation Model Development' section. F_{jk}^{HC} and F_{jk}^{LC} are determined from the polynomial response surface equations of the surrogate model, as stated in Eqs. (6) and (7), respectively.

Heavy Vacuum Gas Oil (HVGO) Yield

The objective function of maximising HVGO yield is expressed as

$$\text{Maximise } F^{\mathrm{HVGO,Tot}} = \sum_{j=1}^{J}\sum_{k=1}^{K} F_{jk}^{\mathrm{HVGO}} \tag{20}$$

F_{jk}^{HVGO} is determined using the polynomial response surface equation of the surrogate model, as stated in Eq. (5). This objective function is also subjected to the constraints expressed in Eqs. (9)–(10). By solving the objective function, the maximum HVGO yield, $F^{\mathrm{HVGO,Tot\_max}}$ of VDU with the corresponding optimal crude blending ratio and operating conditions is determined. Besides, the TAC with respect to the maximum HVGO yield is calculated using Eqs. (12)–(19), as shown in the 'Total Annualised Cost (TAC)' section.

Pareto-Optimal Solutions

As aforementioned, HVGO yield and TAC contradict. Hence, the trade-off between HVGO yield and TAC is required. This trade-off is determined by introducing the second objective function of TAC, as stated in Eq. (11), and subjected to the constraint of HVGO yield. The constraint of HVGO yield is expressed as below:

$$F^{\mathrm{HVGO,Tot}} \le F^{\mathrm{HVGO,Tot\_max}} \times \theta \tag{21}$$

where θ is the fraction (i.e. 0.90, 0.8, 0.7).

By varying the θ in Eq. (21), a set of optimised HVGO yield and TAC results are obtained as the Pareto-optimal solutions. These Pareto-optimal solutions are used to analyse the relationship between HVGO yield and TAC which develop physical insight for the decision-makers to decide upon a preferred solution.

Case Study

In this section, a case study is presented to illustrate the methodology that is discussed in the 'Methodology' section. The case study aims to determine the optimal crude blending composition with their respective operating conditions that simultaneously give maximum HVGO yield and minimum TAC. Three different types of crude oil blending, such as heavy-light, heavy-medium, and heavy-medium-light, are compared and analysed in this case study. The application of the proposed methodology in the case study is explained in the following sub-sections.

Development of Simulation Model

The crude assays, namely light crude (33.99 API), medium crude (28.79 API), and heavy crude (28.21 API), are selected as the feedstock. The properties of each crude oil, including the true boiling point data and light end analysis, are analysed and presented in Tables 3 and 4, respectively.

Table 3 Crude oil properties

	Light crude	Medium crude	Heavy crude
Density (lb/ft^3)	53.27	55.00	55.2
API gravity (°API)	33.99	28.79	28.21
Light end analysis (wt. %)			
Ethane	0.000	0.000	0.039
Propane	0.146	0.030	0.284
i-Butane	0.127	0.089	0.216
n-Butane	0.702	0.216	0.637
i-Pentane	0.654	0.403	0.696
n-Pentane	1.297	0.876	1.245

Based on the generated working curves, a set of hypothetical pseudo-components are created for each crude oil. With the aid of the oil product cut option, the selected crude oils are blended in different ratios for different types of crude blending in the oil environment of Aspen HYSYS. After blending, the crude oil is installed in the simulation environment. Next, the simulation model of the crude distillation unit is developed based on the operating parameters and column specifications listed in Aspen HYSYS version 10. The listed conditions of this rig column are given in Tables 5 and 6, respectively. After comparing with several thermodynamic fluid packages, the Peng-Robinson equation-of-state is chosen to simulate the crude distillation model. This is because the Peng-Robinson equation of state is the most suitable thermodynamic fluid package to predict the selected crude oil's phase behaviour and volumetric properties. The constructed simulation model is then used to generate the sampling points for developing surrogate models.

Table 4 True boiling point data of the selected crude oil

Cumulative yield (wt. %)	Temperature (°F)		
	Light crude	Medium crude	Heavy crude
0	31	88	27
5	160	180	154
10	236	256	255
20	347	395	400
30	446	504	523
40	545	611	645
50	649	721	770
60	758	840	902
70	876	974	1044
80	1015	1131	1198
90	1205	1328	1381
95	1350	1461	1500

Table 5 Parameters and specifications of the atmospheric distillation column

Parameters and specifications	Value
Total trays	50
Feed tray	40
Kerosene stripper withdraw, return tray	10, 6
Diesel stripper withdraw, return tray	20, 16
AGO stripper withdraw, return tray	30, 26
Kerosene pump-around withdraw, return tray	10, 7
Diesel pump-around withdraw, return tray	20, 17
AGO pump-around withdraw, return tray	30, 27
Condenser pressure (psig)	4
Top pressure (psig)	12
Bottom pressure (psig)	22
Furnace outlet pressure (psig)	25
Total condenser temperature (°F)	130
Top tray temperature (°F)	250
Bottom tray temperature (°F)	650
Furnace outlet temperature (°F)	635

Independent Variables and Process Constraints

The surrogate models are built to represent the relationship between VDU's independent and dependent variables. The superstructure is constructed to develop surrogate models, as shown in Fig. 6.

This superstructure indicated all the possible operating routes and their respective connections in different types of crude blending. These operating routes represented the independent variables that have significant impacts on the dependent variables of VDU. As discussed in the 'Methodology' section, HVGO yield, HVGO pump-around cooler utility flowrate, LVGO, pump-around cooler utility

Table 6 Parameters and specifications of the vacuum distillation column

Parameters and specifications	Value
Total trays	14
Feed tray	12
LVGO withdraw tray	4
HVGO withdraw tray	8
Sop wax withdraw tray	11
LVGO pump-around withdraw, return tray	4, 1
HVGO pump-around withdraw, return tray	8, 5
Top pressure (psig)	− 13.73
Bottom pressure (psig)	− 13.50
Furnace outlet pressure (psig)	− 11.22
Top temperature (°F)	180
Furnace outlet temperature (°F)	760

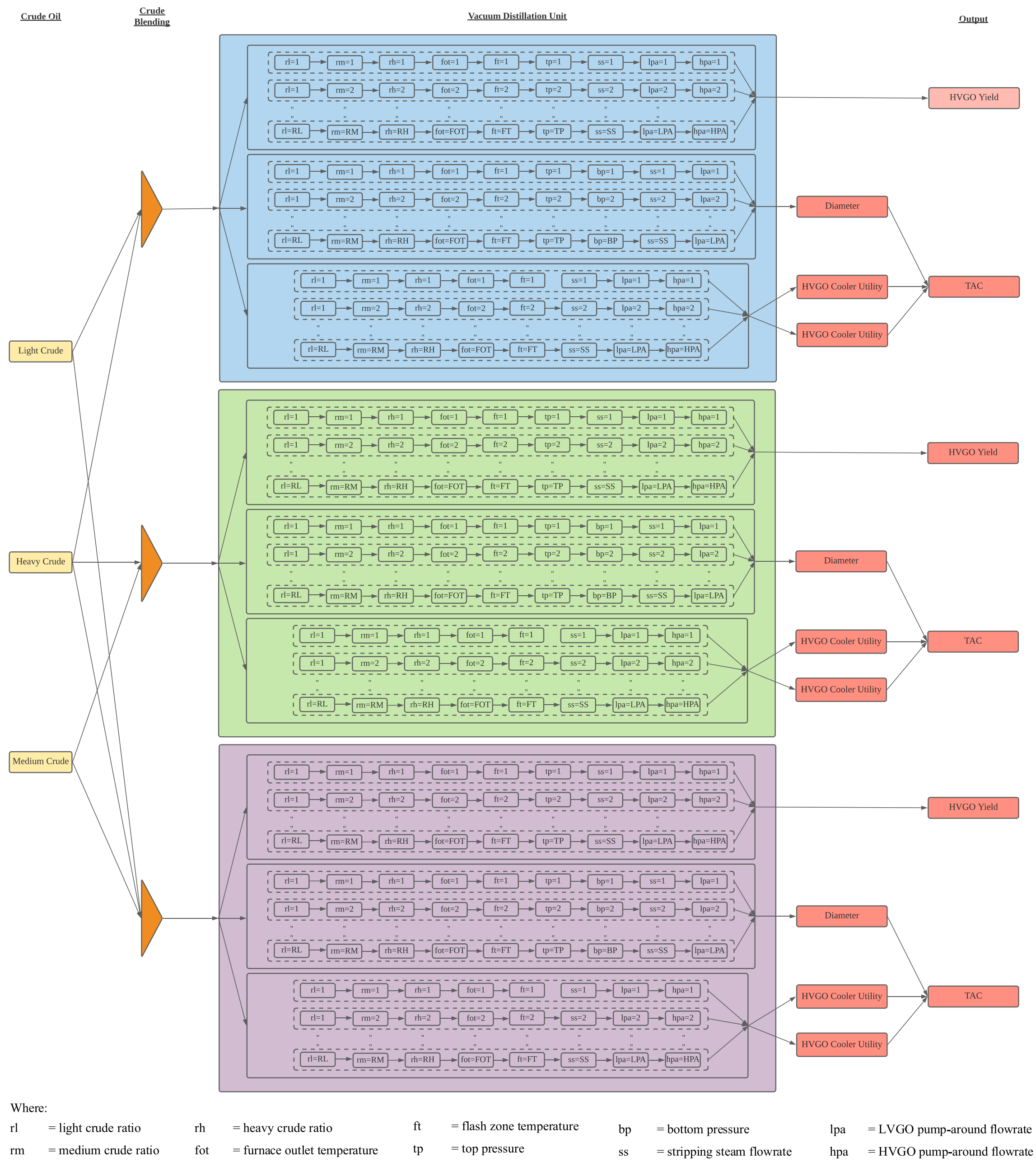

Fig. 6 Superstructure that indicates all the possible operating routes and their respective connections in each type of crude blending

flowrate, and column diameter are chosen as the dependent variables of the surrogate models. Besides, the development of the VDU surrogate model considered the crude oil blending ratio and operating conditions as the independent variables. Three types of crude oil blending are conducted based on different crude blending ratios of light crude ($X_{\text{light},k}$), medium crude ($X_{\text{medium},k}$), and heavy crude ($X_{\text{heavy},k}$). The upper and lower bound limits (i.e. X_{jk}^{U} and X_{jk}^{L}) of each crude oil ratio are given in Table 7. The operating conditions of the case study are varied based on the crude blending ratio. Seven input variables related to the operating conditions are selected. Those variables are furnace outlet temperature (T^{FO}), flash zone temperature

Table 7 Bounds of each crude ratio

Crude blending ratio, X_{jk}	X_{jk}^{L}	X_{jk}^{U}
Light crude ratio	0.2	0.8
Medium crude ratio	0.2	0.8
Heavy crude ratio	0.2	0.8

(T^{FZ}), column top pressure (P^{T}), column bottom pressure (P^{B}), stripping steam flowrate (F^{SS}), HVGO pump-around flowrate (F^{HPA}), and LVGO pump-around flowrate (F^{LPA}). Each variable with the respective lower and upper bound limits (i.e. Q_{jik}^{U} and Q_{jik}^{L}) is summarised in Table 8.

The lower and upper limits of each operating condition are determined by performing a literature review. Note that the lower and upper limits of HVGO and LVGO pump-around flowrate are not reported in the literature. Hence, case studies are conducted in the simulation model to fine-tune the HVGO and LVGO pump-around flowrate limits. Besides, the process constraints are also determined, as given in Table 9. The total crude blending flowrate that is fed into the distillation model is held constant at the value specified in the Aspen HYSYS listed conditions. On the other hand, the pressure drop of VDU is fixed at the maximum value of 25 mmHg, suggested by (Treese et al. 2020). In order to meet the composition specification of the products, ASTM D86 95% cut points for both HVGO and LVGO are set as constant. Consequently, the product flowrate of VDU is allowed to be varied. After determining the independent variables and process constraints, the surrogate models for each independent variable are constructed. The development of surrogate models is further discussed in the 'Surrogate Model Development' section.

Surrogate Model Development

For the development of VDU surrogate models, 654 sets of sampling points are generated from the Aspen HYSYS simulation model developed in the previous section. For each crude oil blending, four polynomial response surface equations are generated based on the abovementioned dependent variables. In the case of heavy-light crude, the sampling points are generated based on the different ratios of the heavy-light crude blends with their respective operating conditions. Then, JMP is used to regress the corresponding data in the polynomial response surface equations for the heavy-light crude blend. The following discussions use one of the dependent variables, HVGO yield, as an example.

Table 9 Process constraints

Constraints	Specifications
Feedstock (barrel/day)	99,000
Column pressure drop (psig)	− 0.49
LVGO ASTM D86 95% recovery (˚F)	915
HVGO ASTM D86 95% recovery (˚F)	1050

The regression results of the HVGO yield in the heavy-light crude blend surrogate model are demonstrated in Figs. 7 and 8 and Table 10. Figure 6 provides the regression coefficients of the crude blending ratio and seven operating variables calculated by JMP version 15. Log-worth value in Fig. 7b is defined as $-\log_{10}(P$ - value). The lower the P-value, the higher the log-worth value. The blue line in Fig. 7b shows the log-worth value of 2. As log-worth value is defined as $-\log_{10}(P$ - value), the blue line is drawn at P-value of 0.01, and it serves as the reference line for comparison of the significance of different parameters. As observed from Fig. 7b, the HVGO pump-around flowrate has influenced the HVGO yield the most, as HVGO pump-around flowrate has the highest log-worth value. This is followed by the light crude ratio, LVGO pump-around flowrate, etc. On the other hand, it can be observed that heavy crude ratio and flash zone temperature have the least but still significant impacts on the HVGO yield. Apart from that, Fig. 8 presents the leverage plots of each independent variable which can help to investigate further the effect of each independent variable on HVGO yield. The effect is significant at the 5% level when the confidence curve (red-coloured line) crosses the hypothesis line (blue-coloured horizontal line). In contrast, the effect is considered insignificant if the confidence curve does not cross the hypothesis line. As observed, the leverage plots suggest that each independent variable significantly impacts HVGO yield. Hence, all the selected independent variables are included in developing the surrogate model. To further validate the model, the R-square of the model must be higher than 0.9. As observed from Table 10, the R-square of the HVGO yield surrogate model is 0.957, confirming that the model has high accuracy. The procedures of the surrogate model development are repeated

Table 8 Bounds of each operating condition

Operating conditions, Q_{jik}	Q_{jik}^{L}	Q_{jik}^{U}	References
Furnace outlet temperature (˚F)	720	780	(Treese et al. 2020)
Flash zone temperature (˚F)	650	750	(Treese et al. 2020)
Top pressure (psig)	− 14.12	− 13.54	Lousdad 2020)
Bottom pressure (psig)	− 13.63	− 13.05	(Treese et al. 2020)
Stripping steam flowrate (lb/h)	15,000	30,000	More et al. 2010)
HVGO pump-around flowrate (barrel/day)	10,000	45,000	-
LVGO pump-around flowrate (barrel/day)	10,000	35,000	-

(a)

Parameter Estimates

Term	Estimate	Std Error	t Ratio	Prob>|t|
Intercept	56123.818	5712.93	9.82	<.0001 *
Light	1562.0907	93.38056	16.73	<.0001 *
Heavy	367.56263	94.60369	3.89	0.0001 *
FOT (F)	-58.37299	9.199737	-6.35	<.0001 *
FZ Temp (F)	31.560426	12.66527	2.49	0.0130 *
Top pressure (mmHg)	2001.3619	275.7731	7.26	<.0001 *
Stripping steam (lb/hr)	-0.058861	0.007541	-7.81	<.0001 *
HVGO Pumparound Flowrate (barrel/day)	0.2460291	0.0025	98.41	<.0001 *
LVGO Pumparound Flowrate (barrel/day)	0.0459819	0.003406	13.50	<.0001 *

(b)

Effect Summary

Source	LogWorth	PValue
HVGO Pumparound Flowrate (barrel/day)	389.954	0.00000
Light	51.717	0.00000
LVGO Pumparound Flowrate (barrel/day)	36.030	0.00000
Stripping steam (lb/hr)	13.621	0.00000
Top pressure (mmHg)	11.944	0.00000
FOT (F)	9.378	0.00000
Heavy	3.948	0.00011
FZ Temp (F)	1.888	0.01296

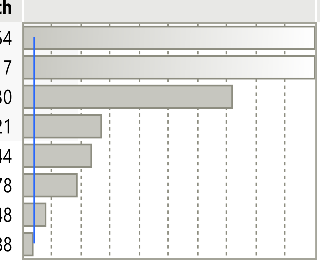

Fig. 7 Regression results of HVGO yield for the heavy-light crude blend that is taken from JMP. **a** Parameter estimates of each selected independent variable. **b** Log-worth value of each selected independent variable

for other dependent variables in the heavy-light crude blend, as well as the dependent variables for the heavy-medium crude blend and heavy-medium-light crude blend. The polynomial response surface equations with the R-square of each dependent variable for all three different types of crude blending are summarised in Table 11. The constructed surrogate models are then integrated into the optimisation model.

Optimisation Model Development

In this section, a multi-objective optimisation model of VDU is formulated using LINGO version 18.0 to determine the trade-off between HVGO yield and TAC. The optimisation work of the VDU has led to mixed-integer nonlinear programming containing linear, nonlinear, and integer variables as well as constraints. The model had a total of 169 variables, 12 nonlinear variables, 3 integer variables, 196 constraints, and 12 nonlinear constraints. This mixed-integer nonlinear programming model aims to maximise the HVGO yield while simultaneously considering minimising the TAC. Based on the previous surrogate model development, four polynomial response surface equations of the surrogate model are generated for heavy-light crude blend, heavy medium crude blend, and heavy-medium-light crude blend, respectively. The HVGO yield surrogate model is integrated into the optimisation model to address the objective function of maximising HVGO yield. Meanwhile, the other three surrogate models are incorporated in the optimisation model to address the objective function of minimising TAC. To achieve the objective functions, all the surrogate model equations of the three types of crude blending are incorporated in the optimisation model. In this model, two stages of optimisation procedures are being considered. This includes (a) maximise HVGO yield under varying the crude oil blending ratio and operating conditions and (b) minimise TAC under varying the crude oil blending ratio and varying the operating conditions and constraints on the HVGO yield.

To maximise the HVGO yield of VDU, the objective function shown in Eq. (20) is used. For each type of crude blending, the $F^{\mathrm{HVGO,Tot}}$ is represented by the HVGO yield surrogate model equation, as shown in Table 11. As discussed previously, the surrogate models' crude oil blending ratio and operating variables are subjected to the bound limits. The bound limits of each variable are discussed and given in Table 7 and 8, respectively. By solving the objective function of maximising HVGO yield, subjected to the constraints shown in Eqs. (9) and (10), the optimisation model decided the type of crude blending that gives the maximum HVGO yield, $F^{\mathrm{HVGO,Tot\_max}}$. The corresponding TAC with respect to the maximum HVGO yield is calculated based on Eqs. (12)–(19). For the capital cost calculation, D_{jk}^{col} is represented by the column diameter surrogate model equations, as shown in Table 11. The column wall thickness t_{jk}^{w} is calculated using the equation proposed by Towler and Sinnott (2012), as evaluated below:

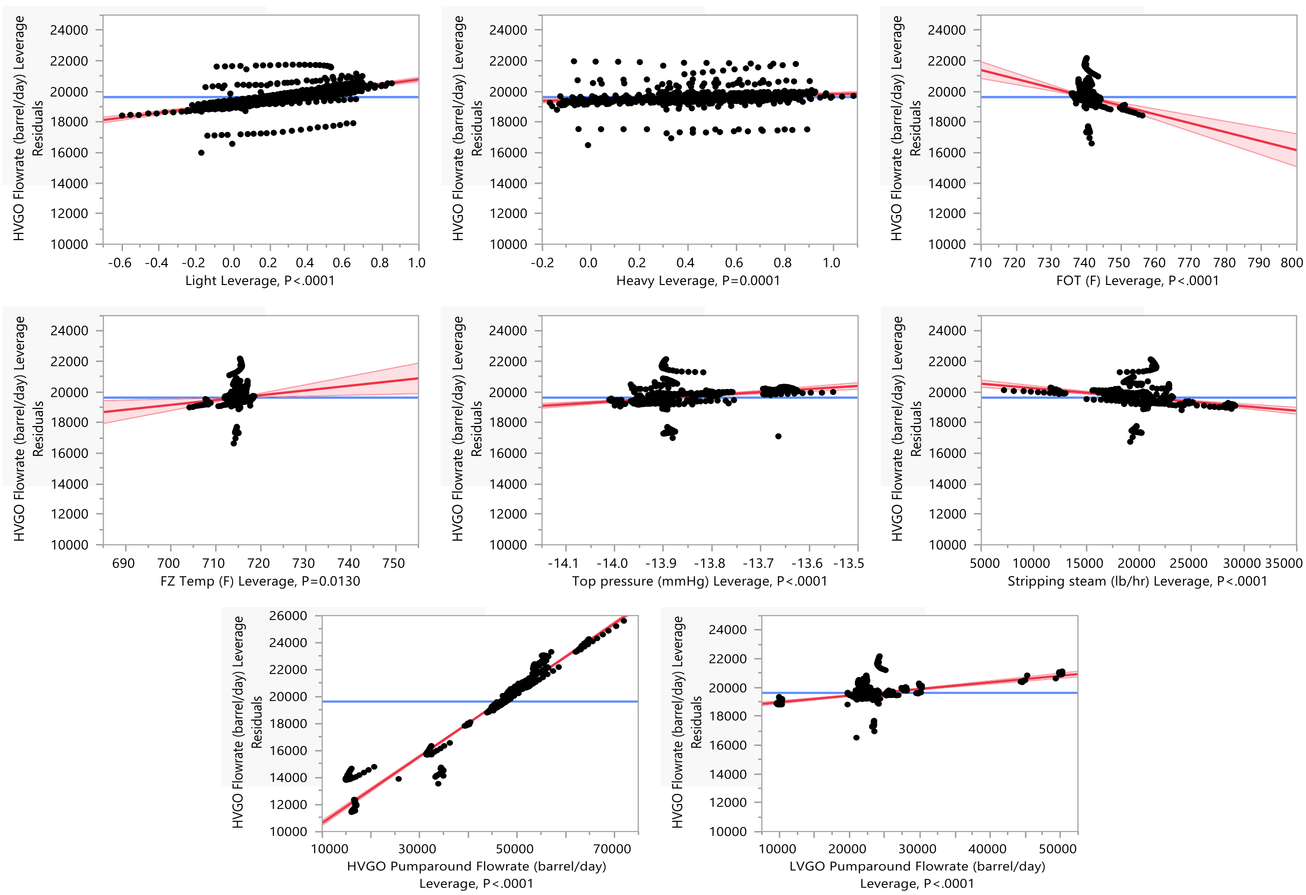

Fig. 8 Leverage plots of HVGO yield for the heavy-light crude blend that is taken from JMP

Table 10 Summary of fit of HVGO yield for the heavy-light crude that is taken from JMP

Summary of fit	Value
R-squared	0.9573
Adjusted *R*-squared	0.9568
Root mean square error	636.5115
Mean of response	19,630.41
Observations	654

Eq. (19). In this work, the operating cost calculation considered the cost of stripping steam entering the VDU as well as the cooling water cost of HVGO and LVGO pump-around coolers. The costs of stripping steam and cooling water are given in Table 12.

After obtaining the maximum HVGO yield, the next step is to minimise the TAC. The objective function in Eq. (11) is implemented in the optimisation model, subjected to the constraints shown in Eq. (21). By varying the fraction from 0.9 to 0.2, a set of Pareto-optimal solutions with the

$$\text{Wall thickness} = \frac{\text{Bottom pressure} \times \text{column diameter}}{2 \times \text{maximum allowable stress} \times \text{weld joint efficiency} - 1.2 \times \text{bottom pressure}} \tag{34}$$

Assuming stainless steel is used as the construction material of VDU, the maximum allowable stress is 89 N/mm^2. Besides, the weld joint efficiency is assumed as 1. The bottom pressure is obtained from the optimised results given by the model. Meanwhile, the operating cost is calculated based on

corresponding optimal crude blending ratio and operating conditions are obtained. The results of the optimisation model with respect to these two objective functions are further discussed in the next section.

Table 11 Polynomial response surface equations of surrogate models in crude blending types 1, 2, and 3

Crude blending type 1: heavy-light crude blend	R^2
$F^{\mathrm{HVGO,Tot}} = 56,124.8176b_k + 1562.0907X^{\mathrm{L}} + 367.5626X^{\mathrm{H}} - 58.3730T^{\mathrm{FO}} + 31.5604T^{\mathrm{FZ}} + 2001.3619P^{\mathrm{T}} - 0.0589F^{\mathrm{SS}} + 0.2460F^{\mathrm{HPA}} + 0.0460F^{\mathrm{LPA}}$ (22)	0.957
$F^{\mathrm{HU,Tot}} = -3,033,430.5267b_k - 51,194.6454X^{L} - 83,221.2531X^{\mathrm{H}} + 2786.0077^{\mathrm{FO}} + 1747.5366T^{\mathrm{FZ}} + 2.9022F^{\mathrm{SS}} + 134.2356F^{\mathrm{HPA}} - 2.3363F^{\mathrm{LPA}}$ (23)	0.999
$F^{\mathrm{LU,Tot}} = -10,795,582.5281b_k - 527,200.2308X^{\mathrm{L}} - 289,120.2673X^{\mathrm{H}} + 75,304.2008^{\mathrm{FO}} - 49,585.7419T^{\mathrm{FZ}} + 25.9577F^{\mathrm{SS}} - 116.0152F^{\mathrm{HPA}} + 9.5706F^{\mathrm{LPA}}$ (24)	0.993
$D^{\mathrm{col,Tot}} = -114.7533b_k - 0.2073X^{\mathrm{L}} + 0.0413T^{\mathrm{FO}} - 0.0260T^{\mathrm{FZ}} - 42.5839P^{\mathrm{T}} + 35.0033P^{\mathrm{B}} + 0.0001F^{\mathrm{SS}} + 0.00001F^{\mathrm{LPA}}$ (25)	0.990
Crude blending type 2: heavy-medium crude blend	R^2
$F^{\mathrm{HVGO,Tot}} = 57,685.9083b_k - 1562.0907X^{\mathrm{M}} - 1194.5281X^{\mathrm{H}} - 58.3730T^{\mathrm{FO}} + 31.5604T^{\mathrm{FZ}} + 2001.3619P^{\mathrm{T}} - 0.0589F^{\mathrm{SS}} + 0.2460F^{\mathrm{HPA}} + 0.0460F^{\mathrm{LPA}}$ (26)	0.978
$F^{\mathrm{HU,Tot}} = -3,084,624.1721b_k + 51,194.6454X^{\mathrm{M}} - 32,026.6077X^{\mathrm{H}} + 2786.0077^{\mathrm{FO}} + 1747.5366T^{\mathrm{FZ}} + 2.9022F^{\mathrm{SS}} + 134.2356F^{\mathrm{HPA}} - 2.3363F^{\mathrm{LPA}}$ (27)	0.999
$F^{\mathrm{LU,Tot}} = -11,322,782.7589b_k + 527,200.2308X^{\mathrm{M}} - 238,079.9635X^{\mathrm{H}} + 75,304.2008^{\mathrm{FO}} - 49,585.7419T^{\mathrm{FZ}} + 25.9577F^{\mathrm{SS}} - 116.0152F^{\mathrm{HPA}} + 9.5706F^{\mathrm{LPA}}$ (28)	0.996
$D^{\mathrm{col,Tot}} = -115.2065b_k + 0.2130X^{\mathrm{M}} + 0.1919T^{\mathrm{FO}} - 0.0254T^{\mathrm{FZ}} - 42.5770P^{\mathrm{T}} + 34.9862P^{\mathrm{B}} + 0.0001F^{\mathrm{SS}} + 0.00001F^{\mathrm{LPA}}$ (29)	0.990
Crude blending type 3: heavy-medium-light crude blend	R^2
$F^{\mathrm{HVGO,Tot}} = 56,124.8176b_k + 1562.0907X^{\mathrm{L}} + 367.5626X^{\mathrm{H}} - 58.3730T^{\mathrm{FO}} + 31.5604T^{\mathrm{FZ}} + 2001.3619P^{\mathrm{T}} - 0.0589F^{\mathrm{SS}} + 0.2460F^{\mathrm{HPA}} + 0.0460F^{\mathrm{LPA}}$ (30)	0.957
$F^{\mathrm{HU,Tot}} = -3,033,430.5267b_k - 51,194.6454X^{\mathrm{L}} - 83,221.2531X^{\mathrm{H}} + 2786.0077^{\mathrm{FO}} + 1747.5366T^{\mathrm{FZ}} + 2.9022F^{\mathrm{SS}} + 134.2356F^{\mathrm{HPA}} - 2.3363F^{\mathrm{LPA}}$ (31)	0.999
$F^{\mathrm{LU,Tot}} = -10,795,582.5281b_k - 527,200.2308X^{L} - 289,120.2673X^{\mathrm{H}} + 75,304.2008^{\mathrm{FO}} - 49,585.7419T^{\mathrm{FZ}} + 25.9577F^{\mathrm{SS}} - 116.0152F^{\mathrm{HPA}} + 9.5706F^{\mathrm{LPA}}$ (32)	0.993
$D^{\mathrm{col,Tot}} = -114.7533b_k - 0.2073X^{\mathrm{L}} + 0.0413T^{\mathrm{FO}} - 0.0260T^{\mathrm{FZ}} - 42.5839P^{\mathrm{T}} + 35.0033P^{\mathrm{B}} + 0.0001F^{\mathrm{SS}} + 0.00001F^{\mathrm{LPA}}$ (33)	0.990

Results and Discussion

This section presents a set of Pareto-optimal solutions with the corresponding crude blending ratio and operating conditions. The Pareto-optimal solutions are then tested in the simulation model, and a comparison between these two sets of results is discussed. Finally, a sensitivity analysis is also performed to investigate the impact of the crude blending ratio on HVGO yield and TAC.

Table 12 Utility costs

Utility	Price ($/tonne)
Stripping steam (from direct-fired boilers)	12
Cooling water (from cooling towers)	0.01

Pareto-Optimal Solutions

The optimised results of maximising HVGO yield are illustrated in Fig. 9. As shown, the crude blending has considered a light crude ratio of 0.8 and a heavy crude ratio of 0.2. Hence, it can be proven that heavy-light crude gives the maximum HVGO yield as compared to the other types of crude blending. The impacts of the selected crude blending ratio in giving the optimal operating conditions of the VDU are illustrated in Fig. 9 as well. As shown, the furnace outlet temperature is 720 ˚F, flash zone temperature is 750 ˚F, top pressure is – 13.54 psig, bottom pressure is – 13.05 psig, stripping steam is 15,000 lb/h, HVGO pump-around cooler flowrate is 45,000 barrels/day, and LVGO pump-around cooler flowrate is 35,000 barrels/day. By operating the VDU at these operating conditions with the designated heavy-light crude blending ratio, the VDU produces a maximum HVGO yield of 23,788 barrels/day. The corresponding TAC for the maximum HVGO yield is calculated to be around $ 1.75 million.

Furthermore, a set of Pareto-optimal solutions is obtained by minimising the TAC, subjected to the constraints of HVGO yield. The Pareto-optimal solutions are illustrated in Fig. 10. All the possible optimal solutions with a different trade-off between HVGO and TAC of VDU are determined in the Pareto analysis. The Pareto-optimal solutions shown in Fig. 10 represented the maximum achievable amount of HVGO yield for a particular value of TAC. The results show that the maximum HVGO yield increased with increasing the TAC when the heavy-light crude blend was selected as feedstock. However, when the heavy-medium crude blend is chosen, the maximum amount of HVGO yield decreased with increasing the TAC. The Pareto-optimal solutions also indicated that the most optimal blending ratio of light crude and medium crude to obtain the minimum TAC is 0.8.

Meanwhile, the corresponding crude blending ratio and operating conditions for each optimised solution shown in the Pareto analysis are summarised in Table 13. As observed, by changing the fraction from 0.9 to 0.6, the model indicated that heavy-light crude is the optimal crude blending to give the minimum TAC. The TAC decreased as the fraction decreased. However, starting from fraction 0.5 to 0.2, it is worth noting that heavy-medium crude blending is the optimal crude blending. Besides, TAC increased when the

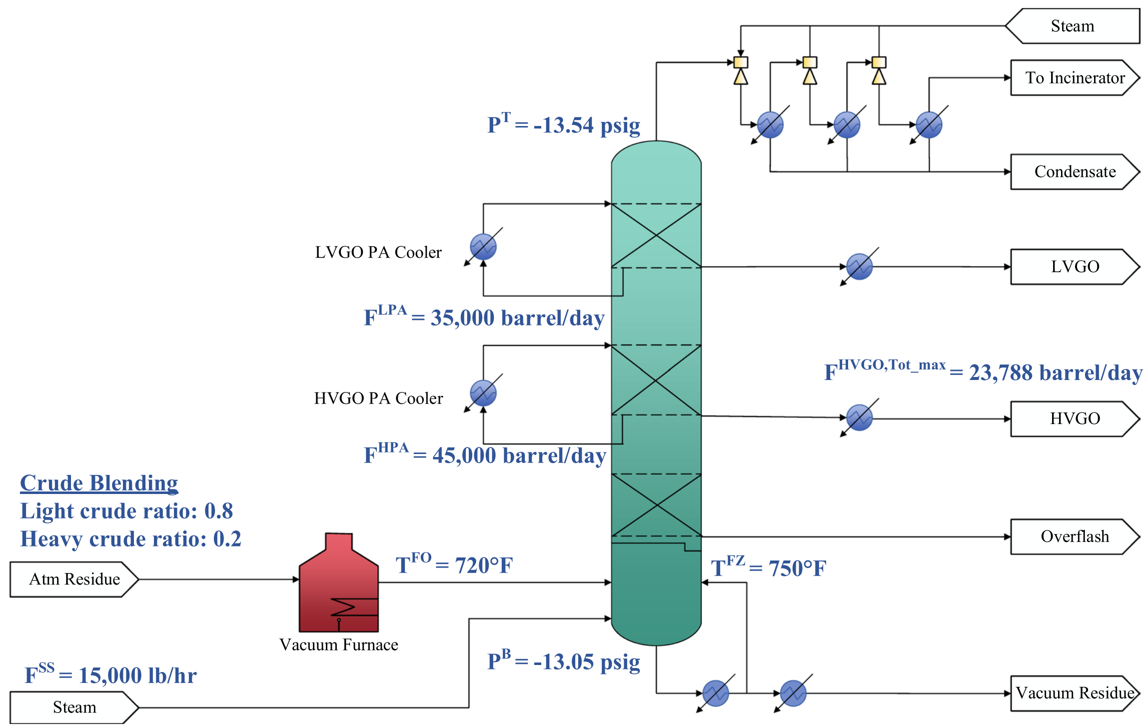

Fig. 9 Optimised results of maximising HVGO yield

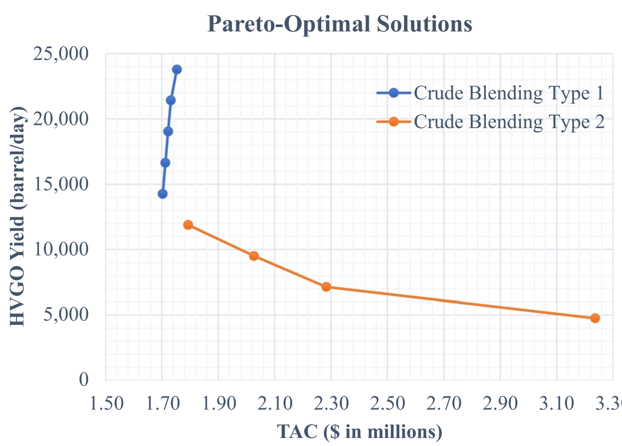

Fig. 10 Pareto-optimal solutions

fraction is further decreased. Of the seven operating variables, only HVGO pump-around flowrate showed a significant change when the fraction is changed from 0.9 to 0.6. However, when the fraction changed from 0.5 to 0.2, HVGO pump-around flowrate did not show any significant change and remained at the variable's lowest bound limit. Similarly, LVGO pump-around flowrate showed no significant change in the Pareto-optimal solutions. Additionally, the furnace outlet temperature stayed at the highest bound limit, starting from fraction 0.3. Further improvement on the HVGO pump-around flowrate, LVGO pump-around flowrate, and furnace outlet temperature can be achieved if the range of the bound limits is widened. However, it is important to note that the range of the limits has already been set by the VDU operational constraints. Therefore, other variables, such as stripping steam and flash zone temperature, are varied by the optimisation model to satisfy the objective functions.

Comparison Between Simulation and Optimisation Model

To validate the accuracy of the optimisation model, the Pareto-optimal solutions obtained from the optimisation model are tested in the simulation model. By using the same optimal crude blending ratio and operating variables given in Table 13, the deviations between two sets of Pareto-optimal solutions are illustrated in Fig. 11.

Based on Fig. 11, crude blending type 1 obtained from the optimisation and simulation models had a similar trend, and only a small deviation is observed between the two sets of results. On the other hand, a big deviation is observed between the two sets of results in crude blending type 2. The ASTM D86 95% cut points of HVGO and LVGO were the main reasons that caused the deviation in crude blending type 2. As mentioned in the 'Independent Variables and Process Constraints' section, ASTM D86 95% cut points of HVGO and LVGO are held constant, so the product flowrate can vary. Hence, another comparison between the simulated and optimisation results is made

Table 13 Corresponding results for optimised values shown in Pareto analysis

θ	1.0	0.9	0.8	0.7	0.6	0.5	0.4	0.3	0.2
Type of crude blending	1	1	1	1	1	2	2	2	2
Light crude fraction	0.8	0.8	0.8	0.8	0.8	0	0	0	0
Medium crude fraction	0	0	0	0	0	0.8	0.8	0.8	0.8
Heavy crude fraction	0.2	0.2	0.2	0.2	0.2	0.2	0.2	0.2	0.2
Furnace outlet temperature (˚F)	720	720	720	720	720	722	763	780	780
Flash zone temperature (˚F)	750	750	750	750	750	750	750	706	650
Top pressure (mmHg)	− 13.54	− 13.54	− 13.54	− 13.54	− 13.54	− 13.92	− 13.92	− 13.92	− 13.92
Bottom pressure (mmHg)	− 13.05	− 13.05	− 13.05	− 13.05	− 13.05	− 13.43	− 13.43	− 13.43	− 13.43
Stripping steam flowrate (lb/h)	15,000	15,000	15,000	15,000	15,000	15,000	15,000	15,000	25,216
HVGO pump-around flowrate (barrel/day)	45,000	40,004	30,335	20,666	10,997	10,000	10,000	10,000	10,000
LVGO pump-around flowrate (barrel/day)	35,000	10,000	10,000	10,000	10,000	10,000	10,000	10,000	10,000

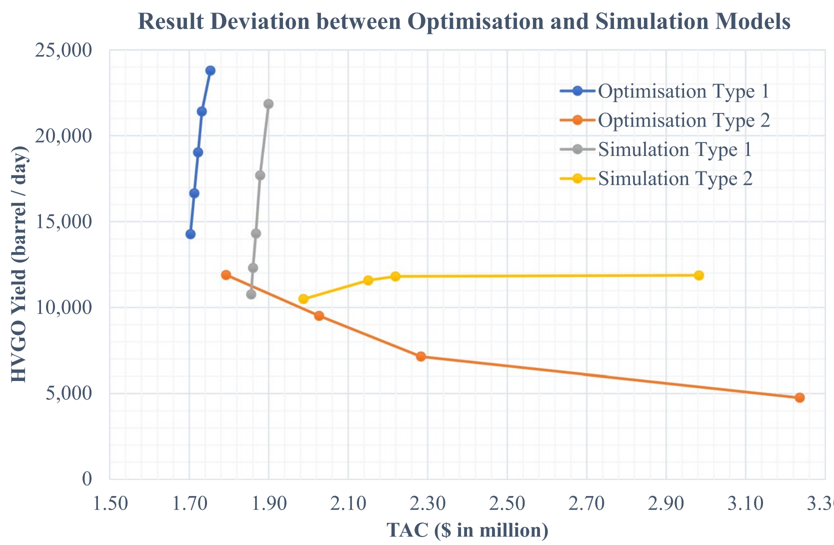

Fig. 11 Comparison of Pareto-optimal solutions between optimisation model and simulation model

by varying the ASTM D86 95% cut points of HVGO. In this comparison, the HVGO flowrate is held constant at the value obtained from the Pareto-optimal solutions, as given in Table 13. The new comparison results are illustrated in Fig. 12.

As shown, the deviation between the two sets of results in crude blending type 2 is very small, and the trends are very similar. However, varying the cut point cannot be done for crude blending type 1. This is because the changes in crude blending type 1 are very limited as the ASTM D86 95% cut point of HVGO has reached the maximum value at the given HVGO flowrate. Thus, a small test is then performed further to validate the accuracy of crude blending type 1 results, as shown in Table 14. By manipulating the operating conditions away from the optimal operating conditions shown in the Pareto analysis, the simulation results showed that the HVGO yield and TAC were not better than the values given in Pareto-optimal solutions. Hence, it can be concluded that the optimisation model still provided an optimised result even though the result has deviated compared to the results given by the simulation model.

Moreover, these optimised results can provide insights into the optimal operating conditions of VDU. The insight allows the integration of the surrogate-assisted mathematical optimisation model into large-scale applications in the refinery. Doing so can help the refiners develop effective strategic planning applications for the VDU operation (Geoffrion 1976). The developed insight can also help overcome the current limitations such as tighter crude demand and fluctuation of crude oil prices in the refinery. Apart from that, the optimisation model can be used to perform computational experiments to help avoid costly mistakes in building pilot-scale plants. In terms of flexibility, the proposed surrogate-assisted mathematical optimisation model can be extended to other equipment or industries. This can be done by incorporating the proposed methodology to develop the surrogate models based on the statistical data of the equipment or industry. Then, the next thing is to develop a new

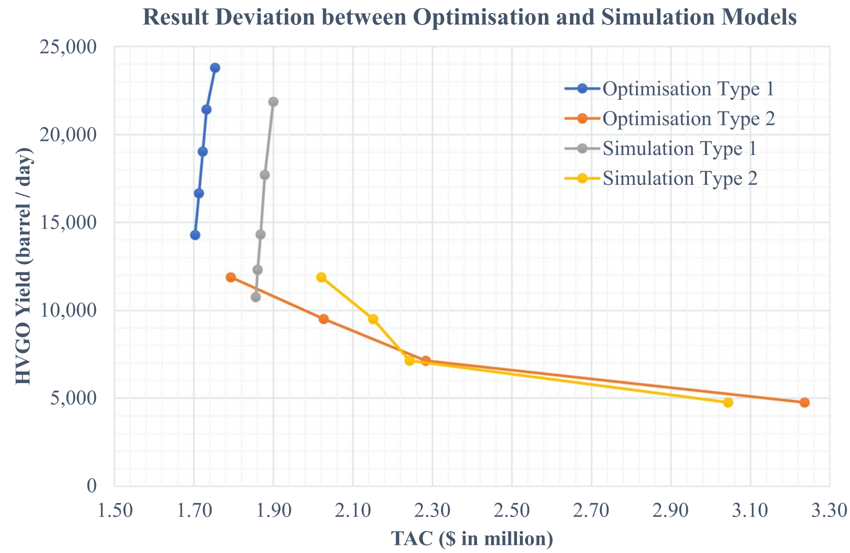

Fig. 12 Comparison of results between optimisation and simulation models by varying the HVGO cut point

Table 14 Tested results to validate the accuracy of crude blending type 1 optimised results

θ	1.0
Light crude fraction	0.8
Medium crude fraction	0
Heavy crude fraction	0.2
Furnace outlet temperature (˚F)	760
Flash zone temperature (˚F)	723
Top pressure (mmHg)	− 13.92
Bottom pressure (mmHg)	− 13.43
Stripping steam flowrate (lb/h)	20,000
HVGO pump-around flowrate (barrel/day)	40,000
LVGO pump-around flowrate (barrel/day)	30,000

optimisation model based on the surrogate models of the equipment or industry.

Sensitivity Analysis on Crude Oil Blending

Sensitivity analysis is carried out to analyse the impact of the crude oil blending ratio on the HVGO yield and TAC. The outcomes of the sensitivity analysis by varying the light and medium crude ratio are shown in Figs. 13 and 14, respectively.

As observed, higher HVGO yield and lower TAC of VDU are provided by the crude blend containing a higher percentage of light crude. It can be concluded that light crude takes a dominant role in the crude oil blending process. This is because light crude contains more distillate and is easier to refine than medium crude. However, light crude tends to have a higher price than medium and heavy crude. Based on the discussions above, crude oil prices are not considered in the operating cost calculations. Thus, Table 15 summarises the prices of the crude blending relevant to the Pareto-optimal solutions. The prices of the crude blending can help to provide further insight for the refiners to decide upon an optimal crude oil blending recipe if they are considering the

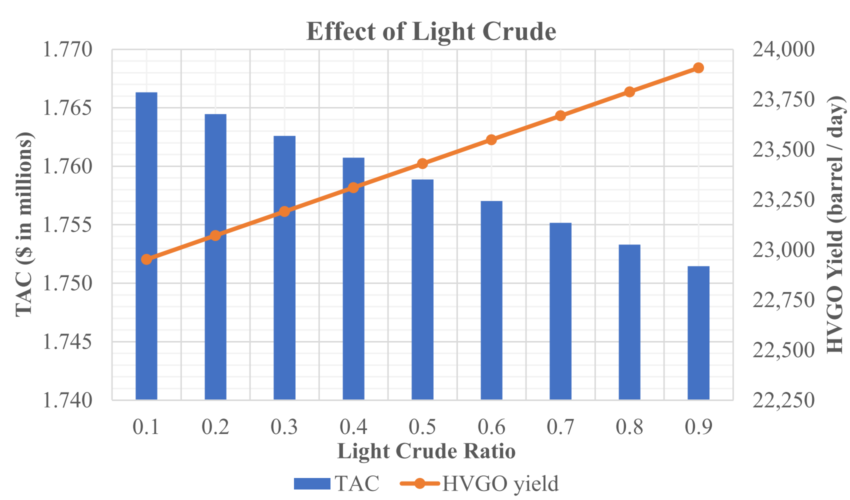

Fig. 13 Impact of light crude ratio on HVGO yield and the total annualised cost of the vacuum distillation unit

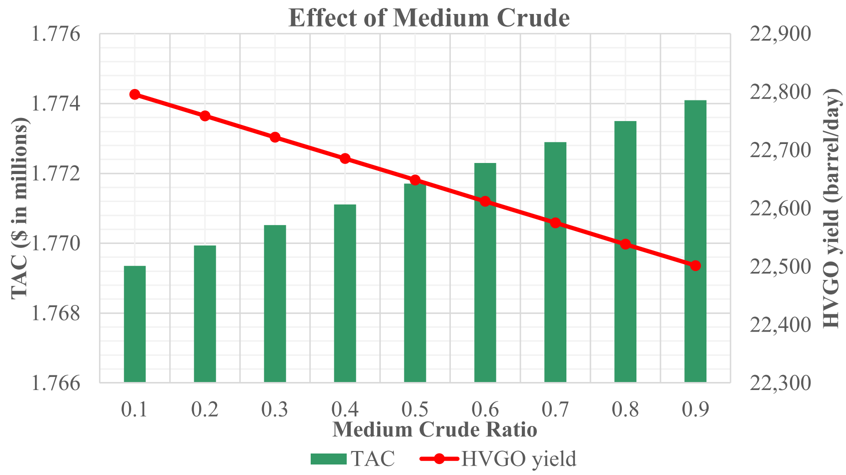

Fig. 14 Impact of medium crude ratio on HVGO yield and the TAC of the vacuum distillation unit

Table 15 Crude blending cost relevant to the Pareto-optimal solutions

θ	1	0.9	0.8	0.7	0.6	0.5	0.4	0.3	0.2
Crude oil prices ($/barrel)	61.90	61.90	61.90	61.90	61.90	61.57	61.57	61.57	61.57

Table 16 Crude oil prices

Crude oil	Price ($/barrel)
Light crude (33.99°API)	62.01
Medium crude (28.79°API)	61.60
Heavy crude (28.21°API)	61.45

prices of crude blending. Meanwhile, the price of each crude oil is given in Table 16.

Conclusion and Future Work

In this work, a surrogate-assisted methodology is developed to capture the relationship between input and output responses of the VDU and thus predicted the complex behaviour of the VDU. The constructed surrogate models are then integrated into the multi-objective mathematical optimisation model to determine the trade-off between HVGO yield and TAC of VDU. The proposed methodology is implemented in a case study where different crude oil blending ratios are compared and analysed. As a result, the heavy-light crude blend ratio of 0.8 provided the maximum HVGO yield as compared to other crude oil blending. The maximum HVGO yield was 23,788 barrels/day and its corresponding TAC was $1.75 million. A set of Pareto-optimal solutions obtained from the optimisation model illustrated the suitable crude blending capable of achieving minimum TAC at each targeted HVGO yield. Besides, comparing the results between the optimisation and simulation models proved that the surrogate-assisted optimisation model can provide accurate estimations of the HVGO yield and TAC. Sensitivity analysis on the crude blending composition is performed, and the results suggested that light crude is the dominant crude in the crude oil blending process. As concluded, the proposed model provided a set of Pareto-optimal solutions that can provide insight for the decision-makers upon deciding on a preferred solution. With this insight, the refiners can easily develop strategic planning procedures to tackle the issues present in the real VDU operation in the refinery.

In the future, the proposed surrogate-assisted methodology can be extended to predict the quality specifications of HVGO. Note that HVGO is the feedstock for the downstream process units in the refinery; thus, it must meet both the downstream units' yield and quality specification requirements. Similarly, the quality specifications of HVGO can be affected by VDU's crude oil composition and operational variables (such as overflash flowrate). Hence, the proposed methodology can be incorporated to maximise the HVGO yield while satisfying the HVGO quality specifications. Additionally, further studies can be carried out to analyse the impact of the number of stages for the distillation columns on the HVGO yield and TAC. Lastly, future work will also focus on using real-time data from the refinery to improve the accuracy of the proposed model.

Abbreviations

CDU: **Crude distillation unit;** ***HVGO***: **Heavy vacuum gas oil;** ***LVGO***: **Light vacuum gas oil;** ***TAC***: **Total annualised cost;** ***VDU***: **Vacuum distillation unit**

Indices

c: **Index for crude feed;** i: **Index for the operating condition in a particular set of the operating conditions;** j: **Index for a**

set of operating conditions; k: Index for crude oil blending model; p: Index for output variables

Parameters

a^{s}, b^{s}: Cost coefficients of column shell; a^{t}, b^{t}: Cost coefficients of tray; C^{rf}: Annualised capital factor; F^{s}: Column shell installation factor; F^{t}: Tray material cost factor; H: Column height; n^{s}: Exponent of column shell; n^{t}: Exponent of tray; N: Number of factors; N^{t}: Total number of trays; r: Interest rate of the return; t: Technology life span; z: Intercept regression coefficient; ρ: Density of material construction; β_{n}: Linear term regression coefficient; β_{ck}: Linear term regression coefficient for X_{ck} in HVGO yield surrogate model equation; α_{ck}: Linear term regression coefficient for X_{ck} in HVGO pump-around cooler utility flowrate surrogate model equation; τ_{ck}: Linear term regression coefficient for X_{ck} in LVGO pump-around cooler utility flowrate surrogate model equation; ε_{ck}: Linear term regression coefficient for X_{ck} in column diameter surrogate model equation; κ_{jik}: Linear term regression coefficients for Q_{jik} in HVGO pump-around cooler utility flowrate surrogate model equation; λ_{jik}: Linear term regression coefficients for Q_{jik} in LVGO pump-around cooler utility flowrate surrogate model equation; σ_{jik}: Linear term regression coefficients for Q_{jik} in column diameter surrogate model equation; ω_{k}: Intercept regression coefficients in HVGO yield surrogate model equation; ϕ_{k}: Intercept regression coefficients in HVGO pump-around cooler utility flowrate surrogate model equation; ϑ_{k}: Intercept regression coefficients in LVGO pump-around cooler utility flowrate surrogate model equation; φ_{k}: Intercept regression coefficients in column diameter surrogate model equation

Variables

ACC: Annualised capital cost; b_{k}: Binary variable; C_{jik}: Utility cost of operating parameters; C_{jk}^{HC}: Utility cost of HVGO pump-around cooler; C_{jk}^{LC}: Utility cost of LVGO pump-around cooler; D_{jk}^{col}: Column diameter; F_{ck}: Flow of crude oil into crude oil blending model; F_{c}^{av}: Availability of crude feed; F_{k}^{Tot}: Total crude blend flowrate; F_{jk}^{HVGO}: HVGO yield; $F^{HVGO,Tot}$: Total HVGO yield; F^{HVGO,Tot_max}: Maximum total HVGO yield; F_{jk}^{HC}: HVGO pump-around cooler utility flowrate; $F^{HC,Tot}$: Total HVGO pump-around cooler utility flowrate; F_{jk}^{LC}: LVGO pump-around cooler utility flowrate; $F^{LC,Tot}$: Total HVGO pump-around cooler utility flowrate; OC: Operating cost; Q_{jik}: Operating conditions; S^{C}: Installed cost of column shell; t_{jk}^{w}: Wall thickness; T^{C}: Installed cost of tray; TAC: Total annualised cost; X: Independent variable; X_{ck}: Crude oil blending ratio; Y: Dependent variable; θ: Fraction

Acknowledgements This work was supported by the School of Engineering and Physical Sciences at Heriot-Watt University Malaysia.

Funding Open Access funding enabled and organized by CAUL and its Member Institutions

Data Availability All data generated or analysed during this study are included in this published article (and its supplementary information files).

Declarations

Conflict of Interest The authors declare no competing interests.

References

Al-mayyahi MA, Hoadley AFA, Smith NE, Rangaiah GP (2011) Investigating the trade-off between operating revenue and CO2 emissions from crude oil distillation using a blend of two crudes. Fuel 90(12):3577–3585

Andiappan V (2017) State-of-the-art review of mathematical optimization approaches for synthesis of energy systems. Process Integr Optim Sustain 1(3):165–188

Aspen HYSYS (2017) Crude tower simulation - HYSYS V10. Aspen Technology Inc: MA

Aydar AY (2018) Utilization of response surface methodology in optimization of extraction of optimization of plant materials. In: Silva V (ed) Statistical approaches with emphasis on design of experiments applied to chemical processes, pp 157–169. IntechOpen

Basak K, Abhilash KS, Ganguly S, Saraf DN (2002) On-line optimization of a crude distillation unit with constraints on product properties. Ind Eng Chem Res 41(6):1557–1568

Chew YE, Putra ZA, Foo DCY (2022) Process simulation and optimisation for acid gas removal system in natural gas processing. J Nat Gas Sci Eng 107. https://doi.org/10.1016/j.jngse.2022.104764

Denimal E, Nechak L, Sinou J, Nacivet S (2016) Kriging surrogate models for predicting the complex eigenvalues of mechanical systems subjected to friction-induced vibration. Shock Vib 2016:22

Foo DCY, Chemmangattuvalappil N, Ng DKS, Elyas R, Chen C-L, Elms RD, Lee H-Y, Chien I-L, Chong S, Chong CH (2017) Chemical

engineering process simulation, 1st edn. Elsevier, Amsterdam, Netherlands
Geoffrion AM (1976) The purpose of mathematical programming is insight, not numbers. Interfaces (providence) 7(1):81–92
Gu W, Huang Y, Wang K, Zhang B, Chen Q, Hui CW (2014) Comparative analysis and evaluation of three crude oil vacuum distillation processes for process selection. Energy 76:559–571
Gu W, Wang K, Huang Y, Zhang B, Chen Q, Hui CW (2015) Energy optimization for a multistage crude oil distillation process. Chem Eng Technol 38(7):1243–1253
Gut JAW, Franzoi RE, Menezes BC, Kelly JD, Grossmann IE (2020) Cutpoint temperature surrogate modeling for distillation yields and properties. Ind Eng Chem Res 59(41):18616–18628
Huang X, Zhao T, Li N, Ma Z, Song L, Li J (2017) Emission-reductive and multi-objective coordinative optimization of binary feed for atmospheric and vacuum distillation unit. Chin Pet Process Pe Technol 19(4):101–112
Ibrahim D, Jobson M, Guille G (2017a) Optimization-based design of crude oil distillation units using rigorous simulation models. Ind Eng Chem Res 56(23):6728–6740
Ibrahim D, Jobson M, Li J, Guillén-gosálbez G (2017b) Surrogate models combined with a support vector machine for the optimized design of a crude oil distillation unit using genetic algorithms. Comput Aided Process Eng 40:481–486
Ibrahim D, Jobson M, Li J, Guill G (2020) Optimal design of flexible heat-integrated crude oil distillation units using surrogate models. Chem Eng Res Des 165:280–297
Inamdar SV, Gupta SK, Saraf DN (2004) Multi-objective optimization of an industrial crude distillation unit using the elitist non-dominated sorting genetic algorithm. Chem Eng Res Des 82(May):611–623
Treese SA, Jones DS, Pujado PR (eds) (2020) Handbook of petroleum processing. Springer Cham
Lund H, Arler F, Østergaard PA, Hvelplund F, Connolly D, Mathiese BV, Karnøe P (2017) Simulation versus optimisation: theoretical positions in energy system modelling. Energies 10:840. https://doi.org/10.3390/en10070840
Li X, Cui C, Sun J (2017) Enhanced product quality in lubricant type vacuum distillation unit by implementing dividing wall column. Chem Eng Process 2018(123):1–11
Liau LCK, Yang TCK, Tsai MT (2004) Expert system of a crude oil distillation unit for process optimization using neural networks. Expert Syst Appl 26(2):247–255
Loper ML (ed) (2015) Modeling and simulation in the systems engineering life cycle: core concepts and accompanying lectures. Springer
López DC, Mahecha CA, Hoyos LJ, Acevedo L, Villamizar JF (2009) Optimization model of a system of crude oil distillation units with heat integration and metamodelling. CT&F-Ciencia, Tecnología y Futuro 3:159–174
López DC, Hoyos LJ, Mahecha CA, Arellano-Garcia H, Wozny G (2013) Optimization model of crude oil distillation units for optimal crude oil blending and operating conditions. Ind Eng Chem Res 52(36):12993–13005
Lousdad S (2020) What is vacuum distillation. https://www.arab-oil-naturalgas.com/what-is-vaccum-distillation/ (accessed 2020–12–20)
Martin GR, Nigg JM (2001) Vacuum pressure control : impact on profitability. Pet Technol Q 6(2):73–81
Mittal V, Zhang J, Yang X, Xu Q (2011) E3 analysis for crude and vacuum distillation system. Chem Eng Technol 34(11):1854–1863
More RK, Bulasara VK, Uppaluri R, Banjara VR (2010) Optimization of crude distillation system using Aspen Plus: effect of binary feed selection on grass-root design. Chem Eng Res Des 88(2):121–134
Motlaghi S, Jalali F, Ahmadabadi MN (2008) An expert system design for a crude oil distillation column with the neural networks model and the process optimization using genetic algorithm framework. Expert Syst Appl 35(4):1540–1545
Ochoa-estopier LM, Jobson M, Smith R (2013) Operational optimization of crude oil distillation systems using artificial neural networks. Comput Chem Eng 59:178–185
Ochoa-Estopier LM, Jobson M (2015) Optimization of heat-integrated crude oil distillation systems. Part III: optimization framework. Ind Eng Chem Res 54(18):5018–5036
Ochoa-Estopier LM, Enríquez-Gutierrez VM, Chen L, Fernández-Ortiz JM, Herrero-Soriano L, Jobson M (2018) Industrial application of surrogate models to optimize crude oil distillation units. Chem Eng Trans 69:289–294
Osuolale FN, Zhang J (2016) Energy efficiency optimization for distillation column using artificial neural network models energy efficiency optimization for distillation column using artificial neural network models. Energy 106(March):562–578
Pintarič ZN, Kravanja Z (2006) Selection of the economic objective function for the optimization of process flow sheets. Ind Eng Chem Res 45(12):4222–4232
Seo JW, Oh M, Lee TH (2000) Design optimisation of crude oil distillation. Chem Eng Technol 23(2):157–164
Tan MC, Foo DCY, Lakshmanan S (2021) An integrated simulation–optimisation approach for free fatty acid removal in palm oil deodorisation process. Asia-Pac J Chem Eng 16(2):e2602. https://doi.org/10.1002/APJ.2602
Towler G, Sinnott R (2012) Chemical engineering design principles, practice and economics of plant and process design Second Edition
Yao H, Chu J (2012) Operational optimization of a simulated atmospheric distillation column using support vector regression models and information analysis. Chem Eng Res Des 90(12):2247–2261